Received: 15 July 2022 | Revised: 12 October 2022 | Accepted: 15 October 2022

DOI: 10.1111/pce.14468

ORIGINAL ARTICLE

Plant, Cell & Environment | WILEY

Ferulic acid is a putative surrender signal to stimulate programmed cell death in grapevines after infection with *Neofusicoccum parvum*

Islam M. Khattab[1,2] | Jochen Fischer[3] | Andrzej Kaźmierczak[4] | Eckhard Thines[3] | Peter Nick[1]

[1]Molecular Cell Biology, Botanical Institute, Karlsruhe Institute of Technology, Karlsruhe, Germany

[2]Department of Horticulture, Faculty of Agriculture, Damanhour University, Damanhour, Egypt

[3]Institut für Biotechnologie und Wirkstoff-Forschung gGmbH, Kaiserslautern, Germany

[4]Department of Cytophysiology, Institute of Experimental Biology, Faculty of Biology and Environmental Protection, University of Łódź, Łódź, Poland

Correspondence
Islam M. Khattab, Molecular Cell Biology, Botanical Institute, Karlsruhe Institute of Technology, Fritz-Haber-Weg 4, 76131 Karlsruhe, Germany.
Email: islam.khattab@kit.edu

Funding information
This study was supported by the European Fund (Interreg Upper Rhine, projects Vitifutur, and DialogProTec). I.M.K. was awarded also a full PhD scholarship from the German Egyptian Research Long-term Scholarships DAAD-GERLS programme in addition to DAAD STIBET grant to complete this study.

Abstract

An apoplectic breakdown from grapevine trunk diseases (GTDs) has become a serious challenge to viticulture as a consequence of drought stress. We hypothesize that fungal aggressiveness is controlled by a chemical communication between the host and colonizing fungus. We introduce the new concept of a 'plant surrender signal' accumulating in host plants under stress and facilitating the aggressive behaviour of the strain *Neofusicoccum parvum* (Bt-67) causing *Botryosphaeriaceae*-related dieback in grapevines. Using a cell-based experimental system (*Vitis* cells) and bioactivity-guided fractionation, we identify *trans*-ferulic acid, a monolignol precursor, as a 'surrender signal'. We show that this signal specifically activates the secretion of the fungal phytotoxin fusicoccin A aglycone. We show further that this phytotoxin, mediated by 14-3-3 proteins, activates programmed cell death in *Vitis* cells. We arrive at a model showing a chemical communication facilitating fusicoccin A secretion that drives necrotrophic behaviour during *Botryosphaeriaceae*–*Vitis* interaction through *trans*-ferulic acid. We thus hypothesize that channelling the phenylpropanoid pathway from this lignin precursor to the *trans*-resveratrol phytoalexin could be a target for future therapy.

KEYWORDS
Apoplexy, Botryosphaeriaceae-related dieback, fusicoccin A, plant surrender signal

1 | INTRODUCTION

Concomitantly with the current climate change, Botryosphaeriaceae-related dieback turned into a progressively devastating threat for viticulture. Around a decade ago, the economic damage by grapevine trunk diseases (GTDs) was estimated to exceed US$1500 million per year (Hofstetter et al., 2012); already in 2016 alone for France, the yield was reduced by 25% corresponding to around US$5000 million (https://www.maladie-du-bois-vigne.fr). The interaction of Botryosphaeriaceae with their grapevine hosts is very complex. The infection process displays two phases—a latent phase linked with reduced vigour of the host that can last very long, and an apoplectic phase during which the host dies off within a few days (Slippers & Wingfield, 2007) as shown in Supporting Information: Figure S1. To what extent the onset of apoplexy is linked with a switch towards necrotrophy remains to be elucidated. This lifestyle is typical of GTDs and differs from other pathogens because it does not meet Koch's postulates defining the criteria for a causative relationship between microbial pathogens and their hosts (Loeffler, 1884). In the case of wood-decaying diseases, there is no strict link between the presence of the microbe and the appearance of disease symptoms. During the endophytic phase, this link seems to be absent; it is a change of fungal behaviour (not the presence of the microbe) that causes apoplexy (Figure 1).

GTDs have always been present in Europe. In fact, the pathogenicity of wood-decaying diseases has been a very ancient phenomenon in vineyards. The first report, written in Arabic, in the book *Kitab Al-Felaha* by the Andalusian Scientist *Ibn Al-Awam* dates back to the twelfth century, and only two centuries later, a Latin description was given in *Opus Ruralium Commodorum* by the scientist *Pietro de' Crescenzi* from Bologna (Mugnai et al., 1999). Nevertheless, the more common outbreak of the symptoms correlates with climate change (Galarneau et al., 2019; Slippers & Wingfield, 2007). Although GTD has been manifest for a long time, we know very little about the molecular mechanisms that provoke a harmless endophyte to turn into a dangerous, toxin-producing killer. Although the impact of plant–pathogen crosstalk in the context of GTDs is clear, we are still far from understanding this crosstalk.

Botryosphaeriaceae-related dieback occurs all over the world and about 21 species of the *Botryosphaeriaceae* associate with dieback in grapevines (Carlucci et al., 2015). The species *Neofusicoccum parvum* has served as an experimental model to study *Botryosphaeriaceae*-related dieback as one of the most aggressive fungal strains (Stempien et al., 2017; Úrbez-Torres & Gubler, 2009).

Visible symptoms appear usually during the advanced stages of the disease. These include cankers in the perennial wood, dead spurs and buds, as well as discolouration of leaves, although these fungi never colonize the leaves of infected grapevines (Mugnai et al., 1999; Úrbez-Torres, 2011). The fungus initiates colonization through wounded wood tissues, usually in the context of pruning (Djoukeng et al., 2009; Úrbez-Torres, 2011). Anatomical investigations showed that the fungus spreads through xylem vessels or parenchymatic rays (Gómez et al., 2016; Khattab et al., 2021; Massonnet et al., 2017).

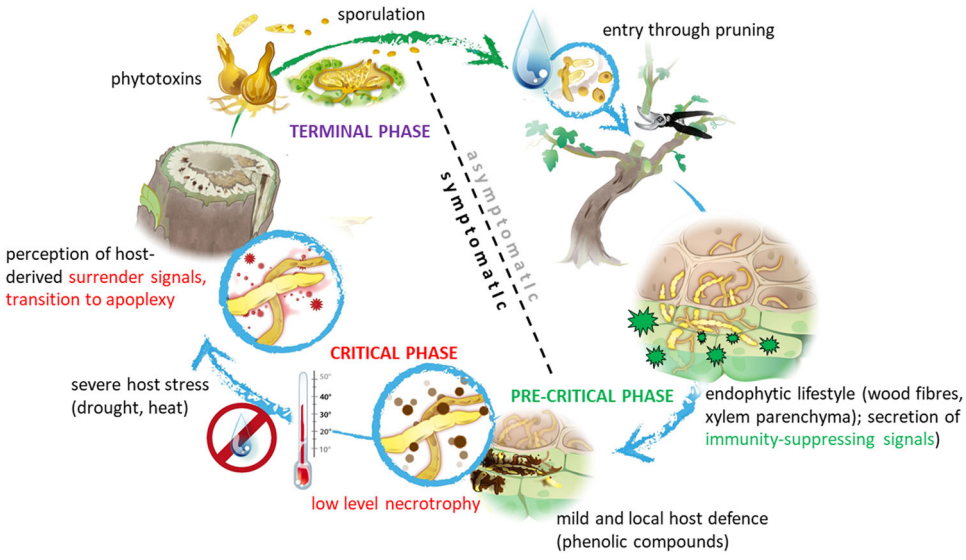

FIGURE 1 Working model on host–pathogen interaction during Vitis–Botryosphaeriaceae dieback used to structure the current study. After entry through pruning wounds, the fungus first colonizes wood fibres and xylem parenchyma and follows an endophytic lifestyle, to a certain extent also showing a transition of necrotrophy at a low level, which is contained by a local and mild defence response of the host (accumulation of phenolic compounds). Host defence is partially quelled by immunity-suppressing signals secreted by the endophyte in a tug-of-war. This precritical phase can last for years and under favourable conditions will not impair the productivity nor vigour of the host. However, if the host is shifted under severe stress such as heat or drought, the critical phase can be initiated. Here, the stress-dependent, chronic loss of physiological homeostasis of the host results in molecular changes that can be perceived by the fungus as surrender signals and activate the transition to apoplexy. This critical phase is, therefore, followed by a terminal phase, where the fungus is producing phytotoxins and initiates sporulation and formation of fruiting bodies resulting in the death of the host and the spread of spores that can colonize neighbouring vines.

Since plants are sessile organisms, efficient immunity responses are mandatory to cope with attacks by invading organisms. Therefore, plant immunity comes in two levels (for a review see Jones & Dangl, 2006; Chuberre et al., 2018). First, a broadband basal immunity acts against entire classes of microbes. Second, a specific immunity, often acting against particular strains of a given pathogen, but not always accompanied by hypersensitive cell death, where infected cells commit to suicide for the sake of the other cells.

Vitis responds to a *Botryosphaeriaceae* infection by activation of genes for phytoalexin biosynthesis and by the accumulation of the respective compounds. However, due to feedback from metabolites to gene activity, both responses are not necessarily parallel. For instance, in several studies, the induction of phytoalexin-related transcripts was not correlated with the degree of susceptibility (Khattab et al., 2021; Labois et al., 2020; Leal et al., 2021; Massonnet et al., 2017). High transcript accumulation was, here, often an indicator of a higher stress level, that is, for susceptibility. Inoculation of *Vitis* plants with *N. parvum* caused a strong decrease in the primary metabolites like sugars, followed by the accumulation of secondary metabolites, such as stilbenes (Labois et al., 2020). This indicates that host metabolism repartitions towards defence compounds. However, this metabolic repartitioning does not necessarily restrict fungal spread. A comparative study with different chemotypes of *V. sylvestris* demonstrated that the higher steady-state transcripts of stilbene synthase genes do not necessarily mean corresponding increases in secondary metabolite abundance. Nevertheless, the efficient containment of the fungus correlates with the local accumulation of specific bioactive phytoalexins, such as viniferin trimers, while glycosylated stilbene species seemed to be irrelevant (Khattab et al., 2021).

With respect to the fungal counteraction, *Botryosphaeriaceae*-related dieback correlates with the secretion of phytotoxic polyketides. Although these compounds seem to be recognized by the host, leading to a defence response, they have to be seen rather as virulence factors, not as elicitors. While it is conceivable that these compounds act as phytotoxins that kill the host cell, before it is able to deploy a defence response, they might also hijack signalling in the host to support a successful invasion. For instance, such signals might induce programmed cell death, which is an efficient defence reaction in the context of a biotrophic pathogen, but counterproductive, if the host cell deals with a necrotrophic pathogen. The fact that the entire secretome of *Botryosphaeriaceae* caused more necrosis in a Chardonnay callus system (Stempien et al., 2017) as compared to the polyketide fraction alone indicates that virulence factors other than polyketides might act as amplifiers. The bioactivity seems to be species-dependent since secretions of *N. parvum* were found to be more aggressive than *Diplodia seriata* (Ramírez-Suero et al., 2014). Indications for a signalling effect come, for instance, from findings that the polyketide terremutin secreted by *N. parvum* not only causes leaf necrosis but also triggers genes regulating flavonoid biosynthesis pathway (Abou-Mansour et al., 2015). The toxic polyketide neoanthraquinone causing drastic shrivelling in *Vitis* leaves is secreted by the related species *N. luteum* (Pescitelli et al., 2020). A widespread compound found across the entire Botryosphaeriacea family is mellein or derivatives thereof, found, for instance, in many *Neofusicoccum* members in Australia and Europe (Andolfi et al., 2011). For instance, Reveglia et al. (2021) have shown that the amount of (*R*)-mellein detected in infected woods was correlated with the amount of the detected fungal DNA. In addition, mellein was described as a virulence factor of *Botryosphaeriaceae*-related dieback, thus increasing disease severity (Trotel-Aziz et al., 2022), although given alone it exerts only a low activity on grapevine leaf discs (Masi et al., 2020).

Botryosphaeria dieback of the host plant is not only correlated to secreted fungal phytotoxins which accumulate in the foliar system following the transpiration stream but also results from the hydraulic failure by tyloses and gelous depositions in the infected vessels (Bortolami et al., 2019; Claverie et al., 2020). For grapevine wilts caused by *Phaeomoniella*, wider xylem vessels were proposed to be linked with susceptibility for apoplectic breakdown, which was linked with a stronger tendency for tyloses and gel pockets allowing the fungus to escape from occluded vessels (Pouzoulet et al., 2017). However, during a comparative study of the spread of *N. parvum*, the fungal spread did not correlate with vessel diameter but was rather dependent on differential channelling of the stilbene pathway (Khattab et al., 2021). Moreover, susceptibility was reported to correlate with the abundance of transcripts for key genes of lignin biosynthesis, like caffeic acid *O*-methyltransferase, which catalyses the conversion of *trans*-ferulic acid from caffeic acid (Umezawa, 2010) (https://www.uniprot.org/uniprot/Q06509), consistent with the finding that a higher lignin content represents a hallmark of susceptibility (Khattab et al., 2021).

After a long biotrophic phase, *N. parvum* turns to necrotrophy leading to decreased vigour of the host, and eventually apoplexy. The molecular mechanisms behind this switch in the lifestyle of this 'hemibiotrophic' pathogen are still elusive. However, the outbreak of GTD seems to be strongly correlated to drought stress, accentuated as a consequence of global warming, which holds true for both the Esca syndrome (Lima et al., 2017) and *Botryosphaeriaceae*-related dieback (Galarneau et al., 2019). While the fungus needs to be present to observe symptoms of the disease, it is not a sufficient condition to trigger apoplexy. Since apoplexy is a conditional phenomenon, it might result from altered chemical communication between the plant and the fungus (Figure 1). Compared to true hemibiotrophs, *Botryosphaeriaceae* fungi seem to represent an evolutionarily ancestral stage of necrotrophy, since they can live as saprotrophs in the wood over many years, before, but turning into necrotrophs and, in the terminal stage, inducing apoplexy. Before the actual apoplexy, during the so-called precritical phase, the fungus colonizes the wood as an endophyte, using cell-wall-degrading enzymes, and the host plant responds by synthesis of phytoalexins. Under climate-borne stress, the fungus leaves the precritical phase culminating in the apoplectic breakdown of the host. The weakened defence response of the host, possibly along with the metabolic changes in the plant evoked by the abiotic stress, allows the fungus to sense a future limitation of resources, which alters the fungal strategy. In response to these metabolic changes in the host changes, the fungus releases distinct polyketides acting as virulence factors for the necrotrophic, terminal phase. Thus, it is the metabolic state of the plant seems to condition the aggressiveness of the pathogen.

In the present study, we test the hypothesis that the *Botryosphaeriaceae*-related dieback in grapevines results from a chemical communication between host and pathogen. We used *N. parvum* Bt-

67 as one of the most aggressive and virulent fungal strains causing this disease (Guan et al., 2016; Stempien et al., 2017). We developed a cell-based experimental system to study plant–fungal interaction in vitro. This experimental system allowed us to screen candidate plant compounds that accumulate under drought stress and can trigger the release of fungal compounds with the strongest phytotoxic activity. We first identified the lignin precursor ferulic acid as a specific and efficient activator for the release of fungal phytotoxins. Using bioactivity-guided fractionation, we were then able to identify a fusicoccin A (FCA) aglycone as bona fide candidate for the strong phytotoxic effect. In the third part of the study, we analysed the mode of action of FCA and found that this compound induced programmed cell death in grapevine cells. Our study aims to show that in the context of host–hemibiotrophic interaction under external stress, the fungus benefits from the plant responses to complete the infectious process.

2 | MATERIALS AND METHODS

2.1 | Plant and fungal materials

The used fungal strain in the study, *N. parvum Bt-67*, was kindly provided by Laboratoire Vigne Biotechnologies et Environnement, Université de Haute-Alsace, France and isolated by Instituto Superior de Agronomia, Universidade de Lisbona, Portugal (Reis et al., 2016; Stempien et al., 2017). We conducted the experiments with the grapevine suspension line Vrup-TuB6-GFP, deriving from *Vitis rupestris*, and expressing an N-terminal fusion of GFP with β-tubulin 6 (Guan et al., 2015). The response of actin filaments was followed using a cell line in *V. vinifera* cv. Chardonnay expressing a florescent fimbrin actin-binding domain 2 (*At*FABD2)–GFP (Akaberi et al., 2018). In addition, two transgenic lines in tobacco (*Nicotiana tabacum* L. cv. 'Bright-Yellow 2' overexpressing *V. rupestris* metacaspases 2 and 5 were used along with their nontransformed wild type (WT); Gong et al., 2019). All cells were subcultured in weekly intervals into Murashige and Skoog medium. The transgenic lines remained under selective pressure by the appropriate antibiotics. All experiments were conducted with cells that were not cycling, either because they had already entered the expansion phase (4 days post subculture for the grapevine cell lines) or were still in the lag phase before the first division (1 day post subculture of tobacco BY-2 cells).

2.2 | Screening the effect of monolignol precursors on *N. parvum* aggressiveness

To probe whether the monolignol precursors cinnamic acid, *p*-coumaric acid, caffeic acid and *trans*-ferulic acid can induce *N. parvum* to secrete phytotoxic compounds, fungal mycelia were fermented with different concentrations (0.5, 1 and 1.5 mM) for each of the mentioned monolignol precursors. Fungal mycelia, grown for 2 weeks on potato dextrose agar (Sigma-Aldrich), were cultivated with the respective compound in 250 ml of 20 g L^{-1} malt extract medium (Carl Roth GmbH), pH 5.3, for 2 additional weeks. After sterile filtration through a 0.22-µm polyvinylidene fluoride membrane (Carl Roth GmbH), the culture filtrate was added to the Vrup-TuB6 cells (35 µl filtrate per ml cell suspension) to test for a potential phytotoxic effect.

To explore whether phytotoxic compounds might be retained inside the hyphae without being secreted, we extracted fungal metabolites, either from medium or mycelia, after 24 h fermentation with the respective precursor after the fungus consumed entirely the sugar, which was checked with a Diabur 5000 test strip (Roche).

2.3 | Extraction of fungal metabolites, HPLC and HPLC-MS analysis for the toxic fraction

The fungus was cultured in a 20-L yeast malt glucose medium (yielding from the culture filtrate about 7.2 g of a crude extract after *trans*-ferulic acid supplement) as explained in Supporting Information: Method S1. Phases of different hydrophobicity (0%, 10%, 20%, 30%, 40%, 50%, 60%, 70%, 80%, 90% and 100% MeCN) were then tested for their bioactivity in the *Vitis* cell culture system. To identify the fungal phytotoxin released in response to *trans*-ferulic acid, the most toxic phase was reanalysed by a high-performance liquid chromatography-mass spectrometry (HPLC-MS) (Series 1200; Agilent) equipped with an UV-diode-array detection and a coupled liquid chromatograph/mass selective detector Trap atmospheric pressure chemical ionization-MS with positive and negative polarization as described by Buckel et al. (2017). For the mass spectrum of the derived molecules as well as their HPLC-MS analysis see Supporting Information: Figure 4. The HPLC-MS analysis of the fraction with the strongest phytotoxicity upon *Vitis* cells identified an FCA aglycone. The FCA signal was verified by an FCA standard, which is part of the IBWF database (CAS 20108-30-9; sc-200754) bought at Santa Cruz Biotechnology, Inc.

2.4 | Mapping the deathly signalling pathway triggered by FCA

After identifying FCA as a fungal phytotoxin, the cellular responses to a synthetic FCA (Santa Cruz Biotechnology) were analysed. We used two concentrations of FCA (6 and 12 µM) to probe the responses of *Vitis* cells, using the line Vrup-TuB6-GFP. To get insight into the cellular events involved in this response, a pharmacological strategy was employed as follows:

2.4.1 | Blocking the FCA receptor, a 14-3-3 protein

Fusicoccin receptors were blocked using BV02 (Sigma-Alrich; Stevers et al., 2018), which inhibits 14-3-3 proteins docking sites as shown in the experimental scheme (Figure 6a). Here, Vrup-Tub6-GFP cells were incubated for 60 min first with 5 µM of BV02, diluted in 100 µM dimethylsulphoxide, before FCA treatment.

2.5 | Inhibiting respiratory burst oxygen homolog (RbOH)

Before FCA treatment, *Vitis* cells were pretreated for 60 min with 1 μM of diphenyleneiodonium chloride (DPI; Sigma-Aldrich), diluted in 100 μM dimethylsulphoxide, which binds to NAD(P)H oxidases in the plasma membrane (PM) as shown in the synthetic scheme (Figure 6e), inhibiting reactive oxygen species (ROS) synthesis in the apoplast (Chang et al., 2011).

2.6 | Measurement of extracellular pH

Changes in the extracellular pH can be used to monitor cellular responses in a noninvasive manner. For instance, activation of PM ATPases will lead to acidification, while the defence-related opening of Ca^{+2} influx channels, by coimport, will lead to alkalinization. This allows us to follow early responses to extracellular signals such as pathogenic mobile polyketides such as mellein and fusicoccin (Guan et al., 2020; Huang et al., 2014; Kesten et al., 2019). Therefore, we followed changes in the extracellular pH in Vrup-TuB6-GFP cells by pH metre (Schott Handylab, pH 12) and recorded by a digital memory recorder displaying the pH at 1-s intervals as detailed in Qiao et al. (2010). To test the effect of blocking 14-3-3 proteins as FCA receptors on ATPase activity, cells were preincubated with 5 μM of the 14-3-3 blocker for 45 min and then treated with FCA (6 μM).

2.7 | Superoxide [O_2^-] detection

ROS play a dual role in biotic stress signalling. They can activate basal defence, or they can induce programmed cell death depending on their temporal relationship with calcium influx (Chang & Nick, 2012). Therefore, we estimated the intracellular superoxide accumulation in *Vitis* cells by the 0.1% (w/v) nitroblue tetrazolium (NBT) assay as described in Steffens and Sauter (2009) and Pietrowska et al. (2014) with modifications. After filtering suspension cells from the culture medium, we incubated the *Vitis* cells in NBT for 1 h under aseptic conditions before washing them in phosphate buffer before observation by bright-field microscopy (Axioskop; Zeiss). Cells accumulating superoxide appeared in blue colour. The frequency of stained cells served as a readout for superoxide accumulation, scoring 600 individual cells for each of three biological replicates of the respective time-point.

2.8 | Live-cell imaging of the cytoskeleton

Since cytoskeletal integrity plays a key role in stress signalling in response to variable pathogen polyketides (Guan et al., 2020; Qiao et al., 2010), we followed the response of the cytoskeleton to FCA using two GFP-tagged marker cell lines. For visualization of microtubules, we employed the marker line Vrup-TuB6-expressing *At*TUB6-GFP (Guan et al., 2015). We observed actin filaments in the marker line from *V. vinifera* cv. 'Chardonnay' expressing Vv-*At*FABD2-GFP (Akaberi et al., 2018), since attempts to engineer an actin-marker cell line in the background of *V. rupestris* have not been successful. The cytoskeletal response was captured by spinning disc confocal microscopy with an AxioObserver Z1 (Zeiss) microscope, equipped with a spinning-disc device (YOKOGAWA CSU-X1 5000) and 488 nm emission light from an Ar-Kr laser (Wang & Nick, 2017). We collected confocal z-stacks, processed them with the ZEN software (Zeiss) and exported them in TIFF format.

To quantify the width of the actin filament, as a readout for actin bundling, which acts as an early hallmark for hypersensitive cell death signalling (Chang et al., 2015; Smertenko & Franklin-Tong, 2011), we transformed the cells of interest into binary images, adjusting the threshold with the B/W option of the ImageJ freeware (https://imagej.nih.gov/ij). Using analyse particles tool, actin filaments were selected automatically. We filtered out random signals by setting the detection threshold to 10 square pixels and using the fit ellipse command to fit the detected particles and to quantify the short ellipse axis as a readout for filament width. The integrity of cortical microtubules was estimated based on the strategy of Schwarzerová et al. (2002). We collected four intensity profiles along the long axis of the cell in equal spacing over the cross axis and using a line width of 25 pixels according to modifications described in Guan et al. (2020). For both microtubule and actin filament quantification, 25 individual cells were scored for each treatment representing four independent biological replicates.

2.9 | Modulation of the cytoskeleton

The cytoskeletal organization was modulated either by stabilization or elimination to investigate its role in the FCA signalling pathway. To assess the role of microtubules on the response to FCA, Vrup-TuB6-GFP were either pretreated with 10 μM of taxol (Sigma-Aldrich), which stabilizes microtubules, or with 10 μM of oryzalin, eliminating microtubules (Sigma-Aldrich) for 30 min, before adding FCA as displayed in the experimental scheme (Figure 7a). To assess the role of the actin filaments, cv. Chardonnay expressing *At*FABD2-GFP marker were pretreated with 2 μM of the actin-eliminating compound latrunculin B (Sigma-Aldrich) for 1 h before FCA treatment as shown in (Figure 8a).

2.10 | RNA extraction and qRT-PCR

V. rupestris (*At*TUB6-GFP) cells were collected and immediately frozen in liquid nitrogen. We extracted total RNA with the RNA Purification Kit (Roboklon). We used 1 μg of total RNA as a template for cDNA synthesis, preincubating with oligo (dT) primers, followed by reverse transcription with M-MuLV enzyme (New England Biolabs) in the presence of RNase inhibitor.

We monitored transcripts of defence-related genes regulating either cell-death signalling or phenylpropanoid pathway and hormone signalling by qRT-PCR using the CFX-PCR System (Bio-Rad) as described in Svyatyna et al. (2014). The housekeeping gene, *EF-1α*,

served to calculate the steady-state transcripts of target genes using the $2^{-\Delta\Delta Ct}$ method (Livak & Schmittgen, 2001). For details of primer sequences and accession numbers of target genes, see Supporting Information: Table S1.

2.11 | Cell death assays

To characterize the type of cell death, we incubated Vrup-TuB6-GFP cells for 2 min with a double staining solution, containing acridine orange (AO) (100 μg ml^{-1}) and ethidium bromide (EB) (100 μg ml^{-1}) (Byczkowska et al., 2013). The stained cells were analysed by fluorescence microscopy (Diaplan, Leitz) upon excitation in the blue (filter set I3, excitation 450–490 nm, beam splitter 510 nm) recording emission above 515 nm and digital image acquisition (Leica DFC 500 and Leica Application Suite, v4). Living cells exclude EB and appear green. Cells in Stage I show the penetration of EB only into the cytoplasm, giving greenish-yellow to yellow nuclei. Cells in Stage II show bright orange nuclei because EB crosses the nuclear envelope. Dead cells lose the AO after the breakdown of the PM, while EB remains sequestered in the DNA, displaying red nuclei. Frequency distributions represent 300–400 individual cells collected from three independent experimental series.

In addition, we used the Evans Blue dye assay (Gaff et al., 1971), which labels dead cells blue as a loss of membrane integrity. We stained the *Vitis* cells with 2.5% Evans Blue (Sigma-Aldrich) for 3 min and then washed twice with distilled water to remove unbound dye. Mortality scores represent populations of at least 1000 individual cells for each biological replicate of the respective treatment.

2.11.1 | In planta infection assay and drought stress

To test the effect of drought stress on disease outbreaks, we followed disease development in infected grapevines under two water regimes in the variety *V. vinifera* cv. 'Augster Weiss' (a male sterile variety often used for genetic introgression, in preparation for future research on resistance breeding), rather than *V. rupestris*, which had been used for the cellular studies, because, here, a fluorescent microtubule marker line was available. After precultivation of wood cuttings for 3 months in pots in the greenhouse, we infected healthy and homogenously grown individuals with *N. parvum* Bt-67 mycelia according to Khattab et al. (2021) and directly subdivided them into two experimental sets. One set was well irrigated 5 days per week and served as control, while the other set developed under constrained irrigation (watering only once weekly). Each set consisted of infected plants and the respective mock control.

2.12 | Fungal colonization and lignin accumulation

We evaluated the result 30 days later for wood necrosis and lignin content according to Khattab et al. (2021) in the infection site, but also at the lower and upper margin of the internode (3 cm below or above the infection site). To evaluate the spread of the fungus through the internodes, we quantified the fungal DNA after extracting genomic DNA from the wood as described in Cota-Sánchez, et al. (2006). We measured the abundance of fungal DNA by qPCR using 25 ng of DNA template, 1 unit of *Taq* polymerase (England Biolabs) and specific internal transcribed spacer (ITS) primers, which bind exclusively to *Botryosphaeriaceae* DNA (Ridgway et al., 2011). For the details of primers and the PCR conditions refer to Supporting Information: Table S1. The abundance of the fungal DNA was evaluated using a calibration curve (Flubacher, 2021), which was calculated based on a dilution series of transformed plasmid DNA amplified by TA cloning in the pGEM®-T Easy vector (Thermo Fisher Scientific) according to the protocol of the producer.

3 | RESULTS

3.1 | Drought stress promotes infection development and lignin accumulation

Since the drought, as accentuated by climate change, seems to promote disease outbreaks, we tested whether restricted irrigation would accentuate the response of grapevines to infection with *N. parvum*. The degree of imposed drought stress was sufficient to induce significant symptoms, that is, reduced growth and partial leaf discolouration (Figure 2a). The wood necrosis due to *N. parvum* Bt-67 infection (Figure 2b, *NP*) was almost twice in the plants under drought stress. To check whether the increase in symptomatic wood under drought stress is related to fungal development, the fungal DNA abundance was quantified 1 month after inoculation using a *Botryosphaeriaceae*-specific *its* for detection (Supporting Information: Method S1 and Figure S2). In fact, we observed that the abundance of fungal DNA was more than twofold increased under drought stress as compared to the control condition in the inoculation site itself, while the two sites 3 cm below or above did not differ.

We also observed that infection induced a significant lignin accumulation. Since drought-induced somewhat more lignin (Figure 2c, W), the lignin content after infection (Figure 2c, NP) was slightly but significantly higher than the value in the infected control. However, there is no indication of a synergistic interaction between infection and drought with respect to lignin deposition, the two factors seemed to act additively.

3.2 | In response to ferulic acid, *N. parvum* secretes an FCA aglycone

Since *N. parvum* aggressiveness depends on plant-derived factors that associate with the stress level of the plant, we tested different monolignol precursors for their ability to elicit the release of fungal factors with toxicity on *Vitis* cells (Figure 2d,e). When we fermented the mycelia in the presence of cinnamic acid and added the culture filtrate to *Vitis* cells, these cells displayed a mortality that was

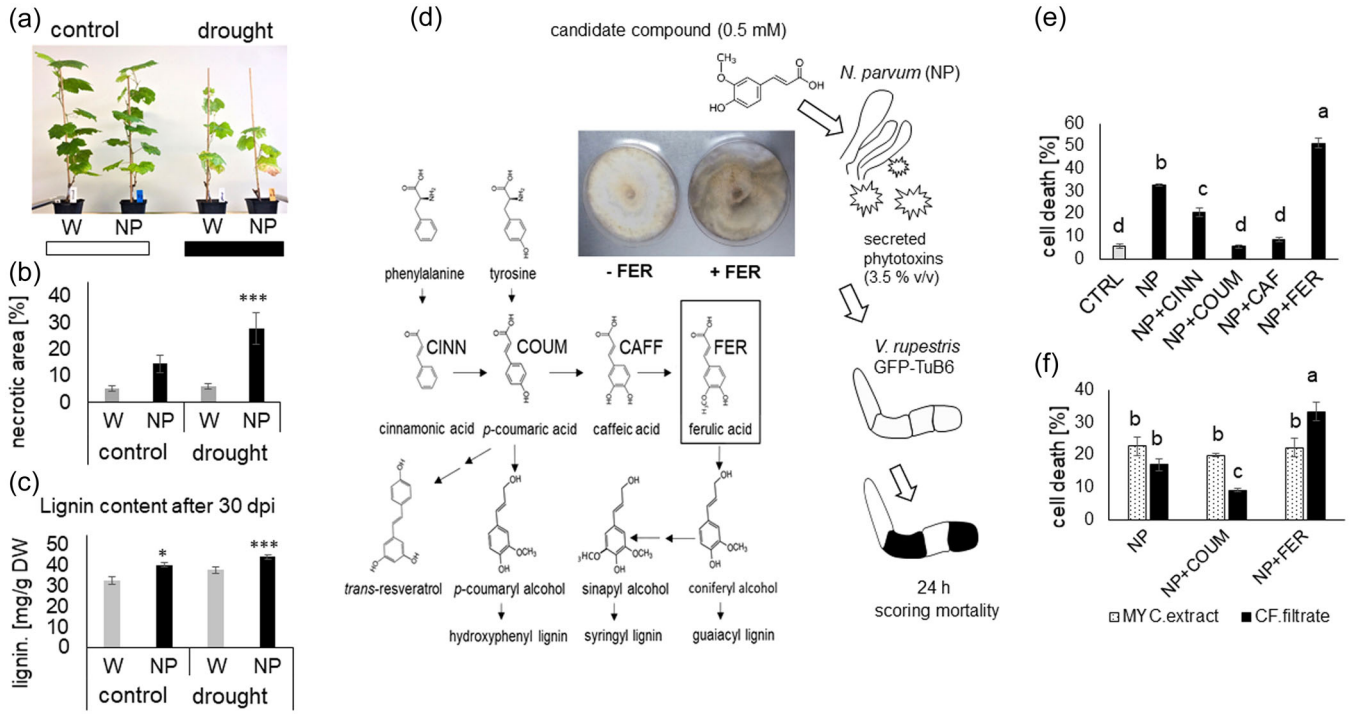

FIGURE 2 Shifting the fungal strain, *Neofusicoccum parvum* Bt-67, to necrotrophic lifestyle. (a–c) Effect of drought stress on fungal development in planta. (a) representative grapevines (*Vitis vinifera* cv. Augster Weiß) raised under either control conditions (optimal water regime) or drought stress (20% of optimal water regime). (b) Coverage of wood necrosis in plants that have been wounded and mock-inoculated (W) versus plants infected with *Neofusicoccum parvum* Bt-67 (NP) 1 month after inoculation. (c) Lignin content at the inoculation site in mock-inoculated versus infected canes 1 month after inoculation. (d) Monolignol pathway showing the positions of cinnamic acid (CINN), *p*-coumaric acid (COUM), caffeic acid (CAFF) and ferulic acid (FER). (e) Experimental design to screen for the surrender signal. Candidate monolignols are fed to *N. parvum* (NP) and the culture filtrate is collected after 2 weeks and added to *V. rupestris* GFP-TuB6 as recipient to screen for phytotoxicity (c). Mortality of the recipient cells scored in response to culture filtrate from *N. parvum* after feeding the fungal donor with different monolignols as compared to culture filtrate from mock-treated cells (NP), or without any filtrate (CTRL). (f) Mortality of the recipient cells in response to fungal metabolites extracted from mycelia (MYC) or recovered from the culture filtrates (CF) after fermentation for 24 h with *p*-coumaric acid or ferulic acid to probe for potential differences in the secretion of the phytotoxins. Data represent means and SE from three independent biological experiments. Asterisks indicate statistical differences by least significant difference test at significance level with $p < 0.05$ (*), $p < 0.01$ (**) and $p < 0.001$ (***) in (b) and (c). Different letters represent statistical differences based on Duncan's test with significant levels $p < 0.05$ in (e) and (f). [Color figure can be viewed at wileyonlinelibrary.com]

significantly lower than the mortality in response to filtrate from untreated mycelium. In a similar manner, supplementation of both *p*-coumaric acid and caffeic acid reduced the toxicity of the fungal culture filtrate reaching the residual mortality levels seen in untreated cells (Figure 2d), irrespective of the precursor concentration (Supporting Information: Figure S3). However, fermenting the mycelia with ferulic acid, a low concentration of 0.5 mM, boosted the toxicity of the culture filtrate, increasing the mortality levels from 32% to 55% (Figure 2e). We observed as well that the mycelia switched to the sexual cycle as evident from excessive spore release when ferulic acid was present in the medium. Asking further whether the difference between ferulic acid and its precursor coumaric acid was due to differences in secretion or to differences in accumulation. To address this, we separated the fungal metabolites secreted to the medium from those remaining inside mycelia. Mycelium extract led to similar mortality rates in the target cells, no matter, whether the mycelium had grown untreated or in presence of *p*-coumaric acid or ferulic acid (Figure 2f). On the other hand, the culture filtrates from the very same cells induced a different mortality: Fermentation in the presence of *p*-coumaric acid produced less phytotoxic culture filtrate than that from *N. parvum* alone, while fermentation with ferulic acid caused higher mortality than the control culture filtrate of *N. parvum* (Figure 2f). This indicates that *p*-coumaric acid and ferulic acid do not differ with respect to their effect on phytotoxin biosynthesis, but with respect to phytotoxin secretion.

To identify the compound responsible for the phytotoxicity, we separated the fungal metabolites based on the hydrophobicity. Hereby, specific peaks only appeared after ferulic treatment and increased, when the hydrophobicity (% MeCN) increased (Figure 3a). These peaks were absent when the fractions originated from fungi fermented in the absence of ferulic acid (Supporting Information: Figure S4). These peaks differed with respect to their hydrophobicity. For instance, a vanillic acid-like compound (Figure 3a, orange box) increased first with rising concentrations of MeCN but was absent in the most hydrophobic fraction (100% MeCN), while a mellein-like compound increased up to 50% MeCN but lacked in 75% and 100%

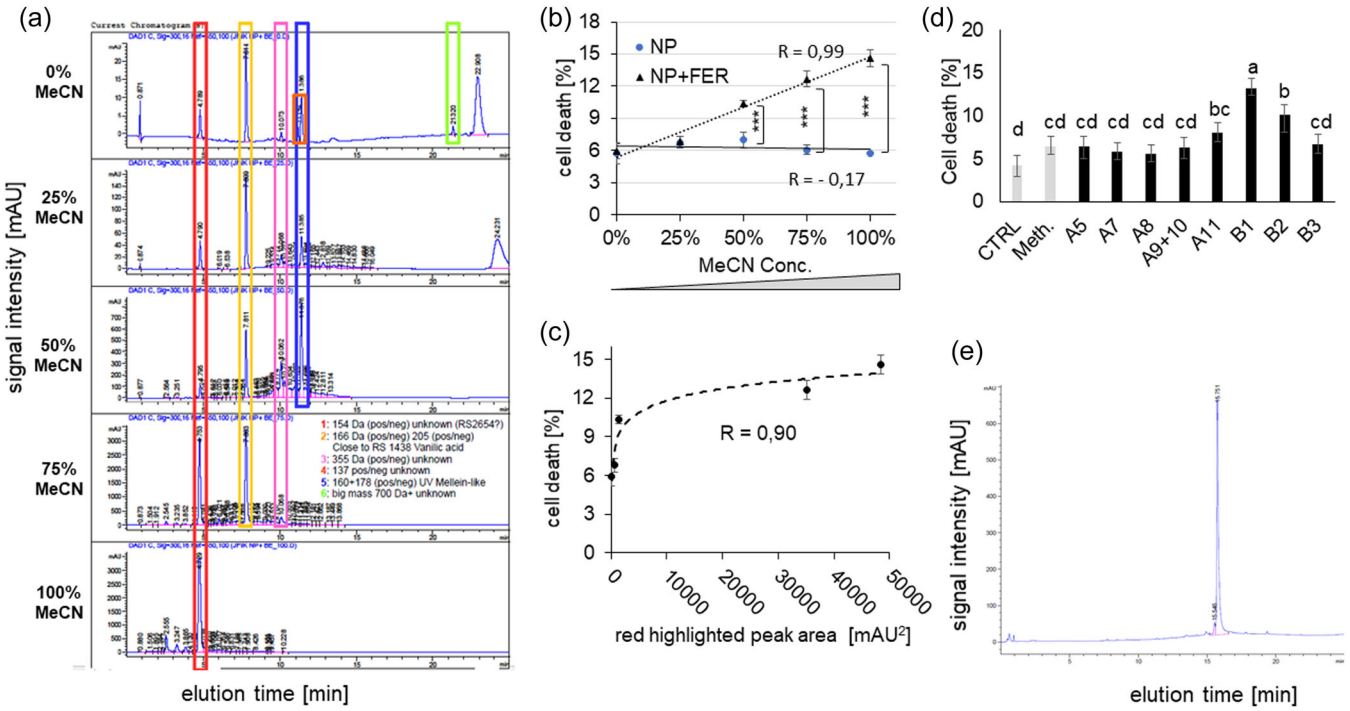

FIGURE 3 Identifying the fungal toxin released in response to fermentation with ferulic acid for 24 h. (a) High-performance liquid chromatography (HPLC) UV readouts for the fungal metabolites secreted by *Neofusicocum parvum* Bt-67 in response to fermentation with 0.5 mM ferulic acid and fractionated using a solid-phase extraction with a gradient of acetonitrile (0%–100% MeCN). (b) Mortality of *Vitis rupestris* GFP-TuB6 suspension cells in response to the fractions from fungal culture filtrates shown in (a). For each fraction, a concentration of 20 µg ml^{-1} *Vitis* cells was administered. (c) Correlation between mortality of the *Vitis* recipient cells and the area for the peak highlighted in (a) by the red box. (d) Mortality of *V. rupestris* GFP-TuB6 cells in response to subfractions obtained from the most hydrophobic fraction of the acetonitrile gradient (MeCN 100%) of *N. parvum* fermented with ferulic acid. Here, a lower concentration (13.3 µg ml^{-1} *Vitis* cells was used, as compared to (b), because the subfractions were more efficient and the material had to be safeguarded for structural elucidation. Mortality was scored after 24 h. (e) A compound isolated from the fraction B1 by liquid chromatography-mass spectrometry analysis and identified as a derivative of fusicoccin A. Bars represent means and SE from three independent experimental series. Asterisks indicate statistical differences by least significant difference test at significance level with $p < 0.05$ (*), $p < 0.01$ (**) and $p < 0.001$ (***) in (b). Different letters represent statistical differences based on Duncan's test with significant levels $p < 0.05$ in (d). [Color figure can be viewed at wileyonlinelibrary.com]

MeCN fractions (Figure 3a, blue box). One peak (Figure 3a, red box, retention time 4.79 min) was prominent because it increased progressively with increasing the hydrophobicity of the extraction. This peak qualified as a bioactive candidate, because the phytotoxicity of the fungal metabolites produced in response to ferulic acid increased with the hydrophobicity of the fraction (Figure 3b), with a very strong correlation ($R = 0.99$). In fact, when we plotted the induced mortality over the area for the peak at a retention time of 4.79 min (Figure 3a, red box), we found a clear saturation curve with a high correlation of $R = 0.9$ (Figure 3c).

Consequently, the most hydrophobic phase was selected for further sub-fractionation by LC and characterization by MS. For the absorption and mass spectra of these subfractions refer to Supporting Information: Figure S5. These fractions from LC were then further tested for their ability to induce mortality in the *Vitis* cells (Figure 2d). Here, the highest bioactivity dwelled in fractions B1 and B2, respectively (Figure 2d). HPLC-MS analysis identified the bioactive compound in the most toxic, fraction B1, as FCA without sugar moiety, FCA aglycone (Figure 3e). In the following, we tried to elucidate the mode of action of FCA.

3.3 | FCA induces autolysis in grapevine cells

To get insight into the quality of mortality induced by FCA, we treated *V. rupestris*, *At*TUB6-GFP cells with either 6 or 12 µM FCA (Figure 4a) and followed the progression of cell death using double staining with AO (membrane-permeable) and EB (membrane-impermeable, DNA binding) to classify the dying cells into different stages as described in the methodology. In response to FCA, the frequency of cells in Stage I and dead cells (Figure 4f) became more abundant. This progression was accelerated for the higher concentration of FCA. The lower dose of 6 µM FCA required 6 h to cause similar mortality as seen for 12 µM FCA at 3 h treatment. Roughly, the velocity of the response increased proportionally with the concentration. The frequency of cells in Stage II was low and mostly constant through all time points. Interestingly, this steady-state level was higher for 6 µM FCA (around 10%–15%) compared with the higher dose (around 5%–10%). Together with the low incidence, this fact indicates that Stage II is short-lived. A cell that is losing the tightness of the nuclear envelope against EB is doomed to timely death. When the response to FCA is speeding up, this will also reduce the steady-state level of Stage II.

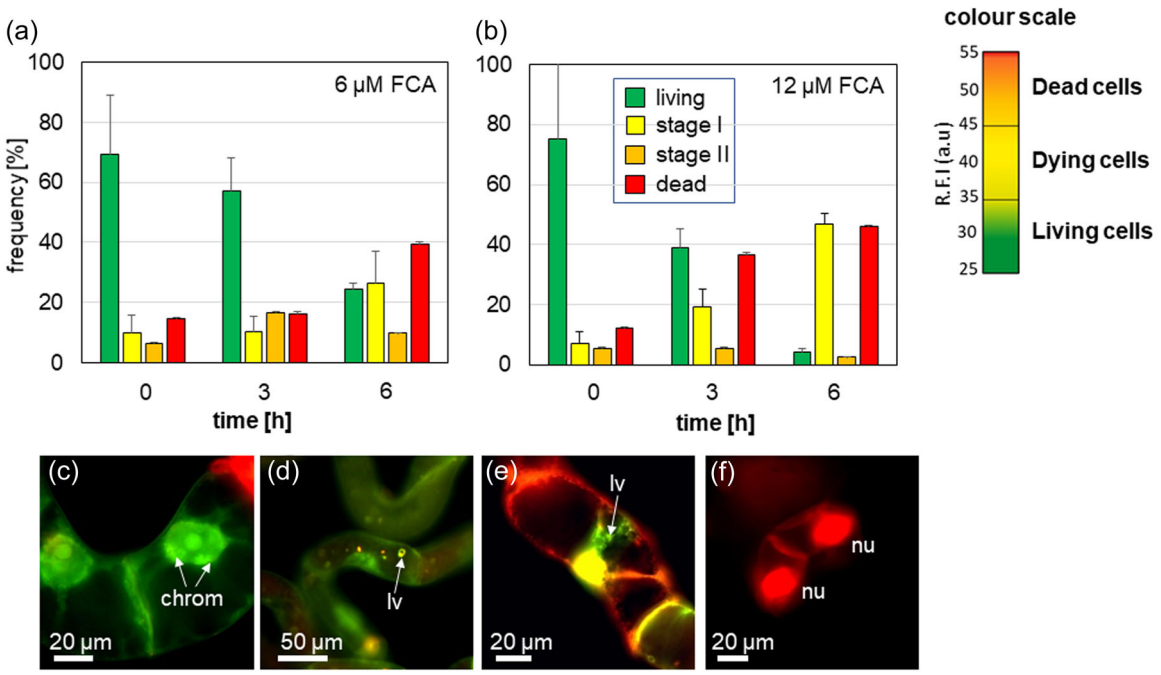

FIGURE 4 Cytological characterization of the cell death in *Vitis* cells in response to fusicoccin A. The cell death response was classified based on double staining with the membrane-permeable fluorochrome Acridine orange (green signal) and the membrane-impermeable fluorochrome ethidium bromide (red signal). Living cells exclude ethidium bromide and appear green, cells in Stage 1 show penetration of ethidium bromide into the cytoplasm, but still exclude the dye from the karyoplasm, cells in Stage 2 show penetration of ethidium bromide into the nucleus, dead cells lose the Acridine orange signal due to complete breakdown of the plasma membrane, while ethidium bromide remains sequestered at the DNA. The frequency of either living, dying or dead cells was calculated based on their fluorescence intensity values (FI) according to the provided colour scale. Time course of these stages in response to 6 µM (a) and 12 µM (b) fusicoccin A. Frequency distributions represent 300–400 individual cells collected from three independent experimental series. (c–f) Progressive stages of autolytic cell death induced by fusicoccin A, such as chromatin condensation in interphase nuclei (c, chrom), or the appearance of lytic vacuoles (lv) in the cytoplasm (d, e). A dead cell void of cytoplasmic signals, but nuclei (nu) labelled by ethidium bromide, representing the terminal stage, is shown in (f). [Color figure can be viewed at wileyonlinelibrary.com]

In addition, this double-staining assay allowed us to observe transitional stages displaying cytological hallmarks of autolytic cell death. For instance, the transition to Stage I was heralded by chromatin condensation (Figure 4c), while progression through Stage I was accompanied by the formation of lytic vacuoles in the cytoplasm of dying cells (Figure 4d,e). In the terminal stage, the nuclei were red, while the cytoplasmic signals observed in dying cells, vanished (Figure 4c–e).

To test whether the response of grapevine cells would be reflected in a corresponding response of grapevine tissues, we administered FCA (9 µM) to leaves through the petiole. In fact, we saw that FCA induced severe leaf necrosis when scored 20 h after the onset of the treatment (Supporting Information: Figure S6). Thus, the death response to FCA also proceeds in cells that are embedded in a tissue context.

3.4 | Response to FCA recapitulates cell-death-related defence

To map the signalling deployed by FCA, we used a concentration of 6 µM. We observed a fast drop in extracellular pH, as it would be expected from the activation of PM proton ATPase. This acidification reached around −0.2 units within 30 min, kept a plateau for another 20 min and then underwent a second round of acidification reaching −0.3 units at 90 min after the addition of FCA (Figure 5a).

To measure RbOH activity in response to FCA, we visualized superoxide by NBT staining. The proportion of cells staining positive for superoxide increased rapidly to around 25% within 1 h after the addition of FCA (Figure 5b), with significant increases over the control level already at the first measurable time-point (10 min). After the peak at 60 min, the frequency of NBT-positive cells dropped but remained elevated (threefold of control cells). This drop might be linked with a loss of membrane integrity as found already substantial in the AO/EB staining (Figure 4a).

To get insight into the FCA signalling pathway, we followed steady-state transcripts levels of potential stress-marker genes in response to FCA, probing 1, 3 and 6 h (Figure 5c). As markers for superoxide scavenging. The transcripts of *Superoxide Dismutase* genes (*MnSOD1* and *CuSOD2*) showed a rapid and steady induction, albeit to a mild extent. Furthermore, *CuSOD1* displayed mild induction of transcripts only transiently, at 3 h by FCA. We also tested two metacaspase genes, *MC2* and *MC5*, that had been identified as

markers for hypersensitive response in the *Vitis–Plasmopara* pathosystem (Gong et al., 2019). Both metacaspase transcripts were rapidly (within 1 h) up-regulated by FCA but differed subsequently. While *MC5* declined later, the level of *MC2* transcripts continued to rise to reach a peak of more than fivefold after 3 h.

The phenylpropanoid pathway gives rise to both monolignols (i.e., the substrate of the fungus) and to stilbenes (i.e., the central phytoalexin in grapevine). The transcripts of *PAL*, the first committed enzyme of the phenylpropanoid pathway, were rapidly and massively (>30-fold) induced by FCA (Figure 5d). Likewise, stilbene-biosynthesis transcripts accumulated significantly (10–20-fold) within 1 h, especially *STS27* and *STS47*. In contrast, the lignin biosynthesis genes, *CAOMT* and *CAD*, did not show any notable induction.

In addition, FCA-challenged cells accumulated more transcripts of specific *JAZ* genes (*JAZ1* and *JAZ9*) (Figure 5d). This indicates the activation of jasmonate signalling as a hallmark of basal defence. To probe the salicylic signalling pathway, the *NPR1* gene was slightly induced. Also, we observed a minor (1.6-fold) induction of *PR10*, while *PR1* was clearly up-regulated (~6-fold).

This analysis shows that FCA induces a rapid extracellular acidification (probably by activating PM-ATPases) and a rapid increase of superoxide (possibly by activating RbOH). This is followed by rapid and massive induction of phytoalexin synthesis transcripts, and phytohormonal signalling (jasmonate and salicylic acid [SA] pathways). In parallel, transcripts for metacaspases involved in hypersensitive cell death are induced. Thus, FCA mimics several aspects of a cell-death response as normally observed in response to a pathogen attack.

3.5 | FCA-triggered PCD requires the activity of 14-3-3 proteins

The activation of PM ATPases by FCA depends on anchoring 14-3-3 proteins. We asked, therefore, whether blocking 14-3-3 proteins by specific inhibitor BV02 (Stevers et al., 2018) would not only inhibit proton ATPase activity but also the signalling culminating in PCD. We observed that pretreatment with BV02 inhibited extracellular acidification in response to FCA (Figure 6b), demonstrating that the inhibitor was active. Pretreatment with BV02 also modulated the transcript levels of stress-marker genes elicited by FCA (Figure 6c). While the induction of transcripts for *JAZ1* by FCA was not altered by pretreatment with BV02, the *STS27* and *STS47* by FCA became clearly amplified ($p < 0.001$). On the other hand, the observed induction of *PAL* and *PR1* by FCA was significantly quelled ($p < 0.001$). Likewise, the induction of metacaspases (*MC2* and *MC5*) by FCA was mitigated ($p < 0.05$ and $p < 0.001$, respectively).

Furthermore, blocking 14-3-3 protein activity by BV02 reduced strongly the mortality from 30% (FCA alone) to 16% for FCA administered after pretreatment with BV02 (Figure 6d). Since the mortality induced by BV02 alone was around 20%, this low mortality meant that BV02 completely eliminated the mortality induced by FCA.

3.6 | Blocking apoplastic oxidative burst modulates FCA signalling

The activation of defence-related PCD is linked with apoplastic oxidative burst originating from RbOH; we tested whether

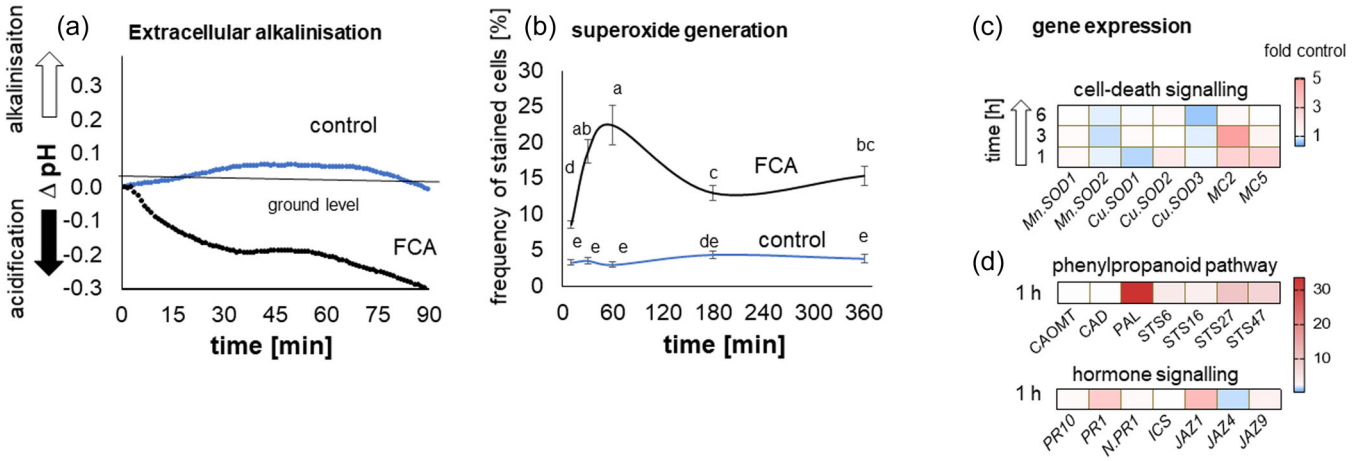

FIGURE 5 Rapid responses of *Vitis rupestris* GFP-TuB6 cells to fusicoccin A (FCA). (a) Activation of plasma-membrane proton ATPases by FCA (6 μM) as detected by acidification of the extracellular medium. (b) Detection of superoxide anions by 0.1% nitroblue tetrazolium. Data represent a population of 600–700 stained cells from three independent experimental series. (c) Modulation of steady-state transcript levels of stress-marker genes measured by qPCR in response to fusococcin A (6 μM) showing steady-state levels for transcripts involved in cell-death signalling such as mitochondrial (*MnSOD*) and plastidic (*CuSOD*) superoxide dismutase genes, as well as defence-related metacaspases (*MC2*, *MC5*) over time. (d) Transcripts of the phenylpropanoid pathway initiating from phenylammonium lyase (*PAL*), exemplarily probing monolignol synthesis (*CAOMT*, *CAD*) and stilbene synthesis (*STS6*, *STS16*, *STS27*, *STS47*). (e) Transcripts of phytohormonal signalling genes (*JAZ1*, *JAZ2*, *JAZ9* for jasmonates; *PR1*, *ICS* for salicylic acid). Colour code represents the significant fold changes of three biological replicates normalized to the control of the respective time-point. Different letters represent statistical differences based on Duncan's test with significant levels $p < 0.05$. [Color figure can be viewed at wileyonlinelibrary.com]

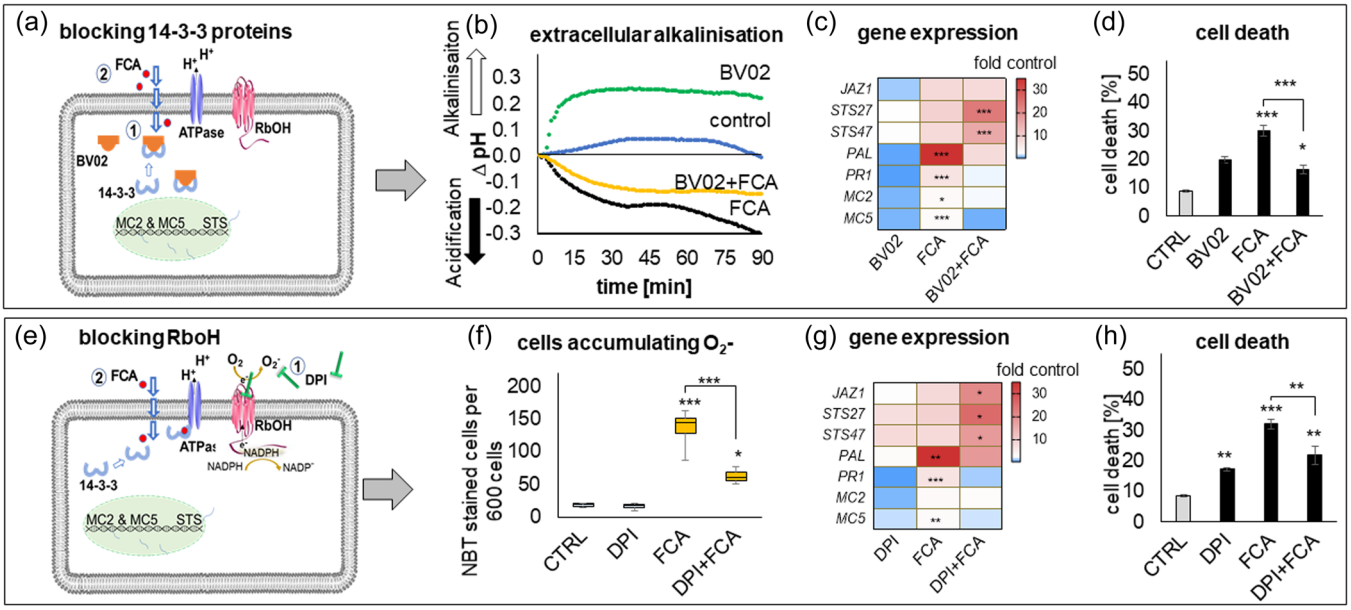

FIGURE 6 Role of 14-3-3 proteins (a–d) and respiratory burst oxygen homolog (RbOH, e–h) for the cellular responses to fusicoccin A (FCA). (a, e) Working model of FCA signalling used to structure the experiments. Response of extracellular acidification as a readout for plasma membrane-localized proton ATPases (b), specific defence-related transcripts (c) and cell death (d) to either 6 μM FCA alone or following a pretreatment with 5 μM of the 14-3-3 inhibitor BV02 for 30 min. As a negative control, BV02 was also tested without the subsequent addition of FCA. Response of superoxide production as a readout for RboH (f), specific defence-related transcripts (g) and cell death (h) to either 6 μM FCA alone or following a pretreatment with 1 μM of the RboH inhibitor diphenyleneiodonium chloride for 60 min. Data represent mean and SE from three independent biological replicates. Asterisks indicate statistical differences by least significant difference test at significance level with $p < 0.05$ (*), $p < 0.01$ (**) and $p < 0.001$ (***). [Color figure can be viewed at wileyonlinelibrary.com]

the FCA signalling can be disrupted by pretreatment with RbOH inhibitor (DPI). In fact, DPI significantly modulated the response to FCA. For instance, pretreatment with DPI significantly reduced the superoxide production in response to FCA by a factor of two (Figure 6f). This was also reflected at the transcript levels for stress-marker genes, albeit in different directions, depending on the gene (Figure 6g). Transcripts of the basal defence genes *JAZ1*, *STS27* and *STS47* were induced by DPI. Likewise, the induction by FCA was more pronounced in presence of DPI. The situation for *PAL* was different. Here, DPI alone induced *PAL* transcripts by about 10-fold. However, the induction by FCA plus DPI was declined to 50% of the level induced by FCA alone. A similar inhibition was observed for the transcripts of *PR1* and *MC5* with significant levels $p < 0.001$ and $p < 0.01$, respectively. In addition, the induction of *MC2* was mildly (but not significantly) inhibited. It should be mentioned that these three transcripts (*PR1*, *MC2* and *MC5*) associated with cell-death-related defence (Chang & Nick, 2012; Gong et al., 2019) were not induced by DPI alone (contrasting with *JAZ1*, *STS27*, *STS47* and *PAL* that are associated with basal immunity). To test whether suppressing the FCA responses of *PR1*, *MC2* and *MC5* would result in a suppression of cell death, we observed that inhibiting RbOH with DPI before FCA treatment significantly reduced the mortality (Figure 6h) to the level seen for DPI treatment alone.

3.7 | Microtubules respond to FCA and modulate FCA signalling

Since microtubules reorganize during defence and since microtubule-directed compounds can modify defence responses (Chang & Nick, 2012), we studied the effect of FCA on microtubules in Vrup-TuB6 cells. FCA eliminated cortical microtubules within 30 min (Figure 7b,f,h). This does not necessarily imply that microtubules participate in FCA signalling because they might respond in a parallel pathway. To dissect this, we stabilized microtubules first with taxol before FCA treatment, which significantly reduced the microtubule elimination by FCA (Figure 7b,g,j). The stabilization of microtubules against FCA was followed by a modulated FCA response of defence-related transcripts (Figure 7c). While taxol enhanced transcripts for genes driving phytoalexin biosynthesis (*PAL*, *STS27* and *STS47*), and significantly amplified induction of these transcripts by FCA, the pattern for *MC2*, *MC5* and *PR1* transcripts differed qualitatively. Here, taxol alone did not induce these transcripts and it significantly inhibited their induction by FCA. Although taxol stabilized microtubules against FCA and modulated the gene expression in response to FCA, it could not mitigate the mortality driven by FCA (Figure 7d). However, comparing the mortality to FCA between our marker line *At*TUB6-GFP (overexpressing β-tubulin), to nontransformed *V. rupestris* cell lines, showed that overexpression of β-tubulin reduced mortality in response to FCA, late to about 25%, at 24 h (Figure 7e). This means that β-tubulin 6 was able to mitigate FCA toxicity.

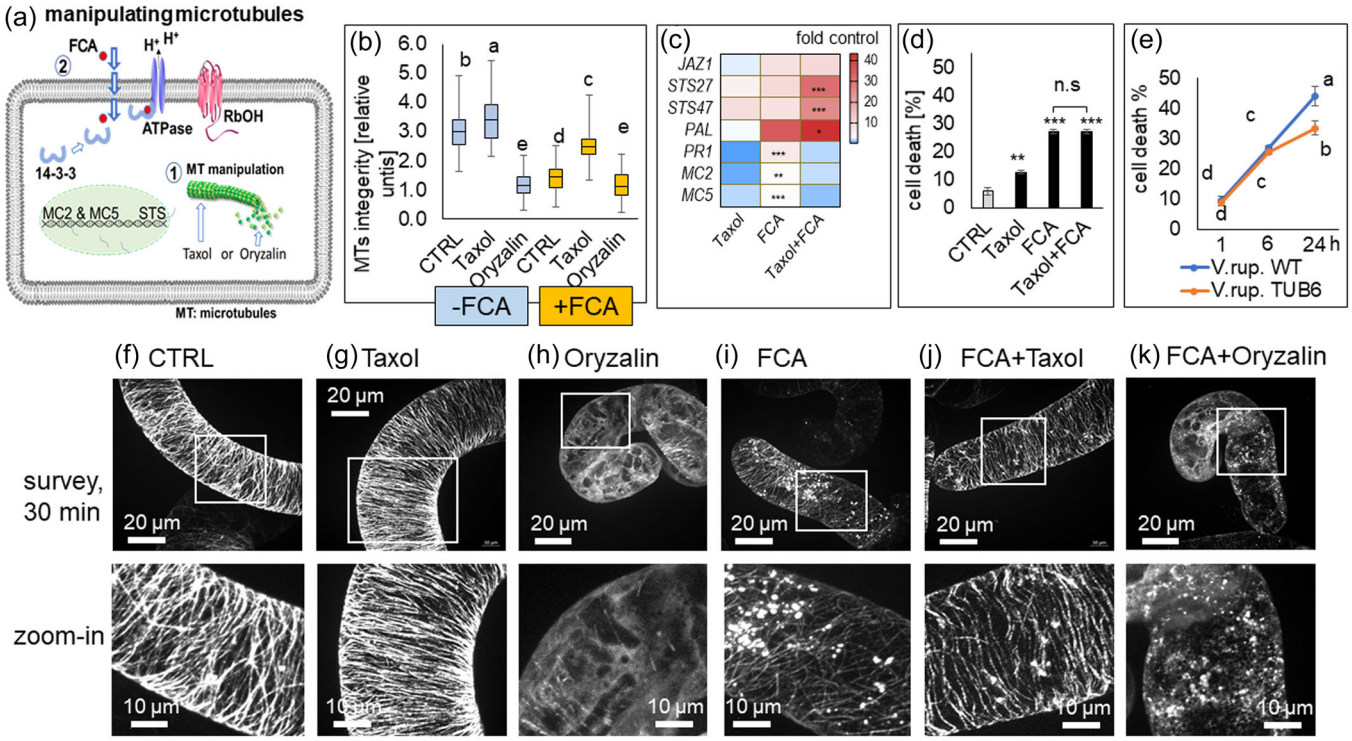

FIGURE 7 Microtubular response to fusicoccin A (FCA) and role of microtubules for the cellular responses to FCA. (a) Working model of FCA signalling used to structure the experiments. (b) Quantification of microtubule integrity for the treatments shown representatively in (f–k). Data represent medians, interquartiles and extreme values for measurements from at least 30 individual cells. (c) Heat map of steady-state transcripts levels for specific defence genes 1 h after addition of 6 µM FCA either alone or in combination with 10 µM taxol. (d) Mortality scored at 6 h after the addition of either 6 µM FCA, 10 µM taxol or a combination of both compounds. (e) Overexpression of microtubules in the *Vitis rupestris* cell line *At*TUB6-GFP mitigates mortality in response to FCA compared to nontransformed *V. rupestris* wild type. Representative *V. rupestris* GFP-TuB6 cells after 30 min of treatment with microtubule-modulating compounds either in the absence (f–h) or in the presence of FCA (d–f). Solvent controls (i–k) 0.1% dimethylsulphoxide, 10 µM taxol (b, e) or 10 µM oryzalin (c, f) are shown. Data represent mean and standard errors from three independent biological experiments comprising 1500 individual cells. Different letters represent statistical differences based on Duncan's test with significant levels $p < 0.05$ in (b) and (e). Asterisks indicate statistical differences by least significant difference test at significance level with $p < 0.05$ (*), $p < 0.01$ (**) and $p < 0.001$ (***) in (c) and (d). ns, Not significant. [Color figure can be viewed at wileyonlinelibrary.com]

To test the effect of microtubule elimination on the mortality response to FCA, we incubated Vrup-TuB6 cells with oryzalin. This strongly depolymerized the microtubules within 30 min (Figure 7b,h). This elimination was seen as well when the oryzalin treatment was followed by the addition of FCA (Figure 7k) without any significant difference between these conditions. Furthermore, the pretreatment of oryzalin did not change the mortality response to FCA (Supporting Information: Figure S7).

Since tubulin overexpression decreases susceptibility to FCA, while microtubule elimination is enhancing, microtubules act as negative regulators for FCA-dependent mortality.

3.8 | Actin filaments respond to and modulate FCA signalling

Since actin filaments are implicated in PCD signalling (for a review see Chang et al., 2015; Smertenko & Franklin-Tong, 2011), we used a grapevine actin-marker cell line expressing (*At*FABD2-GFP) to visualize actin filaments responses to FCA. While in control cells (Figure 8a), actin was organized in a subcortical network of fine strands, it had repartitioned from the cortical network to bundled transvacuolar cables 90 min after FCA addition (Figure 8c). This bundling was significant as seen from measuring bundle width, which was significantly higher in FCA-challenged cells over control cells with $p < 0.001$ (Figure 8e). To probe whether this actin bundling is necessary for FCA-triggered PCD, we eliminated actin strands by latrunculin B pretreatment (Figure 8b). This pretreatment suppressed either the formation of actin cables in response to FCA (Figure 8e) or FCA-dependent mortality to around half the value seen without latrunculin B (Figure 8g). Again, we measured the FCA response of defence-related genes with latrunculin B pretreatment (Figure 8f). Overall, the patterns were similar, but not identical to those seen for taxol pretreatment (Figure 7h). While both latrunculin B and taxol amplified the induction of *STS27* and *STS47* by FCA and both suppressed the induction of *MC5*, the two compounds differed in a couple of points: latrunculin B amplified the FCA response of *JAZ1*, while for *PAL*, latrunculin B partially mitigated the induction by FCA,

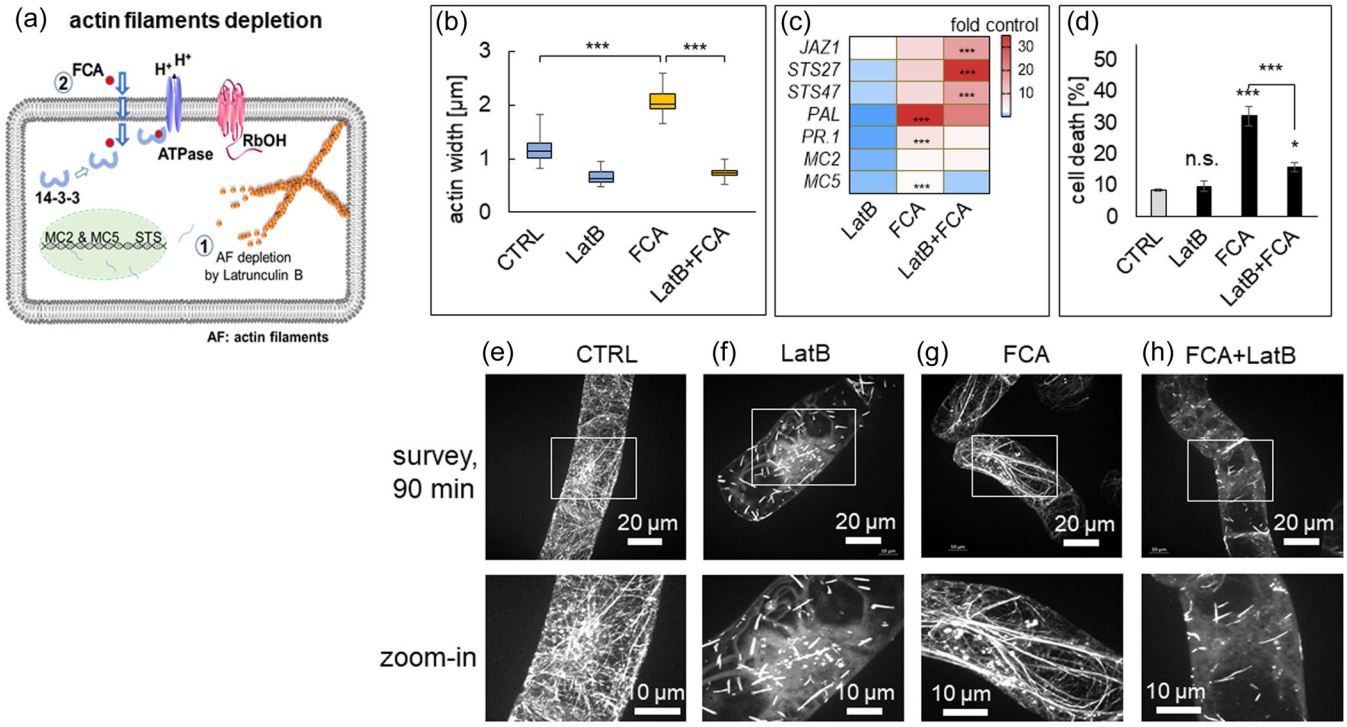

FIGURE 8 Actin response to fusicoccin A (FCA), and role of actin for the cellular responses to FCA (6 µM). (a) Working model of FCA signalling was used to structure the experiments. (b) Quantification of actin bundling for the treatments shown representatively in (e–h). Data represent medians, quartiles and extreme values for measurements from at least 30 individual cells. (c) Heat map of steady-state transcripts levels of stress-marker genes 1 h after the addition of 6 µM FCA either alone or in combination with 2 µM latrunculin B (LatB). (d) Mortality scored at 6 h after the addition of either 6 µM FCA, 2 µM FCA or a combination of both compounds. Representative *Vitis vinifera* cv. Chardonnay FABD2-GFP cells after 90 min of treatment with the actin-eliminating compound LatB (2 µM) in the absence (f) or in the presence of FCA (h), compared to the solvent control (e) 0.1% dimethylsulphoxide, or to FCA alone (g). Data represent mean and standard errors from three independent biological experiments comprising 1500 individual cells. Asterisks indicate statistical differences based on least significant difference test with significant levels $p < 0.05$ (*), $p < 0.01$ (**) and $p < 0.001$ (***). n.s., Not significant. [Color figure can be viewed at wileyonlinelibrary.com]

while taxol amplified it further. Likewise, taxol could clearly suppress the induction of *MC2* and *PR1* by FCA, which was not seen for latrunculin B (Figure 8f). The amplification of *STS27* and *STS47* is of particular interest because the stabilization of microtubules and the elimination of actin strands have the same effect, indicating antagonistic roles of the two components of the cytoskeleton in processing the signal deployed by FCA.

3.9 | Overexpression of metacaspases increased cell death triggered by FCA

In grapevines, defence-related PCD is associated with the up-regulation of two specific metacaspases, *MC2* and *MC5* (Gong et al., 2019). As FCA induced the transcript levels of these metacaspase genes, we tested whether these metacaspases participate in the cell death driven by FCA. For this purpose, we used two BY-2 cell lines overexpressing these metacaspases from *V. rupestris*. In fact, these lines, MC2ox and MC5ox, exhibited a significantly higher mortality in response to FCA, already manifest at the earliest tested time-point, 3 h (Figure 9a). At 6 h, the mortality was tripled (MC2ox) or doubled (MC5ox) compared to nontransformed WT, consistent with a causal role of these metacaspases in executing the cell-death response to FCA.

3.10 | SA mediates FCA-triggered mortality and MAPK cascades seem to be dispensable

SA is often implicated in hypersensitive responses. We tested, therefore, how SA interacts with FCA-induced cell death as described in Supporting Information:Method S1. The pretreatment of SA before the addition of FCA significantly increased mortality from 31% to 44% after 6 h (Figure 9c). Since this result suggested that SA is amplifying the mortality response to FCA, we conducted a parallel experiment, where the synthesis of SA was blocked by pretreatment of 25 µM 1-aminobenzotriazole (ABT) an inhibitor of cytochrome P_{450} oxidases interfering with the phenylalanine-dependent branch of SA biosynthesis through blocking cinnamic acid 4-hydroxylase (Leon et al., 1995). ABT mitigated the mortality induced by FCA, indicating that endogenous SA is involved in the transduction of the FCA effect (Figure 9b). In contrast to SA, manipulation of MAPK

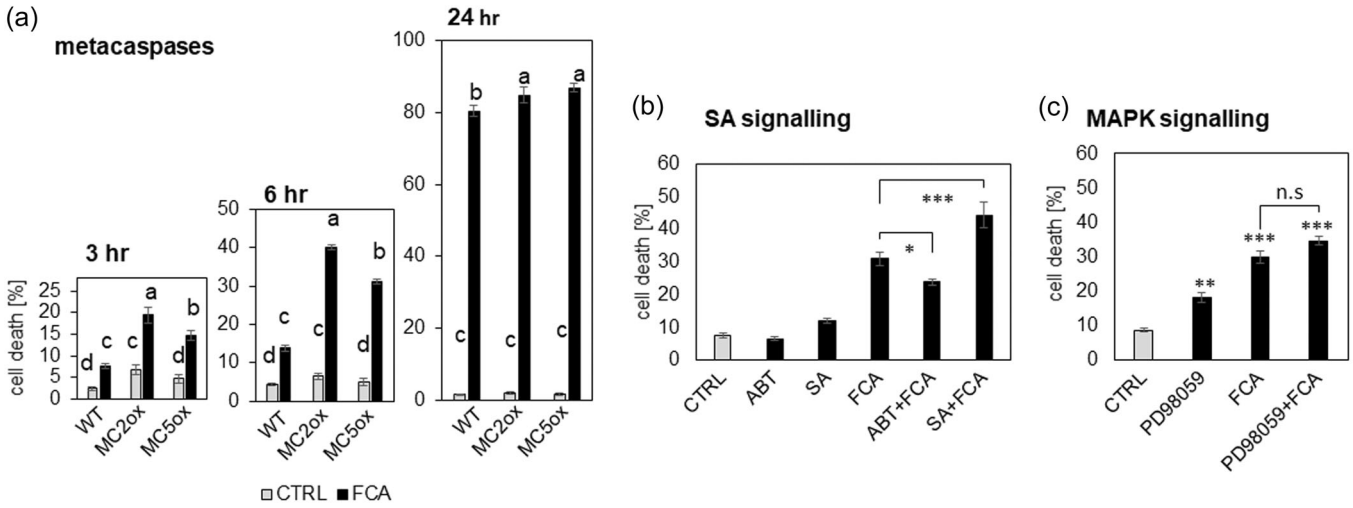

FIGURE 9 Probing for molecular components of the fusicoccin A (FCA) response. (a) Role of metacaspases. Time course of cell death in response to 6 µM FCA in nontransformed tobacco BY-2 cells (WT), and in cells overexpressing either metacaspase 2 (MC2ox) or metacaspase 5 (MC5ox) from *Vitis rupestris*. (b) Role of salicylic acid (SA, 50 µM) and its inhibitor, 1-aminobenzotriazole (ABT, 25 µM) scored 6 h after the addition of 6 µM FCA in *V. rupestris* GFP-TuB6 cells. (c) Role of MAPK signalling. Cell death was scored 6 h after the addition of 6 µM FCA to *Vitis rupestris* GFP-TuB6 cells following pretreatment with 50 µM of the MAPK inhibitor PD98059 for 60 min. Data represent means and SE from three biological replicates comprising 1500 individual cells per data point. Different letters represent statistical differences based on Duncan's test with significant levels $p < 0.05$ (a), asterisks indicate statistical differences based on least significant test with significant levels $p < 0.05$ (*), $p < 0.01$ (**) and $p < 0.001$ (***) in (b) and (c). n.s., Not significant.

signalling by the specific inhibitor PD98059, blocking basal immunity in grapevine (Chang & Nick, 2012), caused mortality levels if given alone (Figure 9c), but was not able to cause significant changes in the mortality response to FCA, indicating that cell death is triggered independently of MAPK.

4 | DISCUSSION

The current work was motivated by a working model, where the fungus changes from an endophytic lifestyle with slow progression of disease symptoms to necrotrophy culminating later by apoplexy of the host, which implies that the endophyte must perceive and respond to input from the host (Figure 1). Those changes in plant metabolism can be used by the fungus to assess and predict the future behaviour of its host, which can be defined as a 'surrender signal' that promotes a transition of the fungus to an aggressive state and favours symptom development. Using a cell-based experimental system based on grapevine suspension cells and the virulent fungus model *N. parvum* Bt-67, we identified this 'surrender signal' as ferulic acid, a monolignol induced under drought stress (Griesser et al., 2015). Ferulic acid (in contrast to its precursor coumaric acid) triggers the fungal release of a phytotoxin, FCA. FCA, secreted by *Fusicoccum amygdali*, was shown to cause severe mortality in sycamore cells (Malerba et al., 2004) and manipulates several cellular responses by initiating the activity of plasma membrane H^+ ATPases over remodelling of actin filaments till the regulation of defence genes (Malerba et al., 2008; Singh & Roberts, 2004). In the first step, we analysed the mode of action of FCA and could show that this fungal compound acts as a signal-evoking PCD in grapevine cells. Thus, FCA release and the host response to this release could result from changes in the chemical communication between the plant and the pathogen upon water stress. As suggested by the model, the fungus would act as a latent endophyte as long as the vine does not meet severe climate-born stress. Challenged by drought, ferulic acid accumulates, which, according to our working model is used by the fungus as a signal conveying a severe loss of metabolic homeostasis of the host, such that it will shift into the necrotrophic phase. Here, this model stimulates the following questions: (1) What renders ferulic acid so specific as a surrender signal under drought stress? (2) By what mechanism can ferulic acid trigger the fungal release of FCA? (3) What is the functional context of FCA-triggered PCD? (4) What does this model contribute to a potential therapy against apoplectic breakdown?

4.1 | By what mechanism can ferulic acid trigger the fungal release of FCA?

The highly potent phytotoxin, FCA, is synthesized by cyclization of geranylgeranyl diphosphate by an unusual diterpene synthase harbouring a C-terminal prenyltransferase domain (Toyomasu et al., 2007). In fact, a homolog with ~60% similarity and all the features of this fusicoccadiene synthase can be located in the *N. parvum* genome

(UniProt ID R1H2L0). How ferulic acid can trigger the release of FCA is not known. However, it is a potent activator of fungal laccases that help the fungus to forage lignin as a carbon source (for a review see Piscitelli et al., 2011). Ferulic acid itself is broken down by feruloyl esterase into vanillin, which is taken up through a specific transporter (Shimizu et al., 2005). Feruloyl esterase can bind the coumaric acid, albeit at a 10-fold reduced affinity; however, it can convert coumaric acid only at a 100-fold reduced velocity (Faulds et al., 2005). Thus, the suppressive activity of coumaric acid on phytotoxin secretion might be caused by coumaric acid blocking the active site of feruloyl esterase. The actual inducer of phytotoxin secretion might therefore be vanillin. In fact, this is supported by our observation that vanillic acid, the oxidized derivative of vanillin, accumulates in the most toxic fraction of fungal exudates (Figure 3a). The transporter for the uptake of vanillin has been already described to be transported to the tip of the growing hyphae through the *Spitzenkörper*, which is also controlling key steps in fungal development, such as the transition from invasive growth towards conidia formation (for a review see Harris, 2009). This would link the foraging of ferulic acid as a food source with developmental switches controlling the aggressive transition during the pathogen lifestyle: from endophytic biotrophy to necrotrophy, later to full apoplexy.

4.2 | Why ferulic acid could be an efficient surrender signal upon drought stress?

The conceptual model used in this study is based on chemical signalling (Figure 1). The chain of events leading to the disease outbreak is promoted by drought stress (Figure 2a), culminating in the accumulation of a plant compound that is utilised by the fungus to assert its aggressiveness. In the search for potential plant compounds that might act as such a 'surrender signal', we focussed on the phenylpropanoid pathway for two reasons: (1) This pathway gives rise to stilbenes, the major phytoalexins in grapevine. (2) It also gives rise to lignin, the major carbon source for the fungus, and commonly accumulates under drought stress (Tu et al., 2020). This response is probably of adaptive nature since the apposition of this hydrophobic compound to the cell wall helps to retain water for transport in the vascular tissue. In our previous study, we could show that the partitioning of the phenylpropanoid pathway between stilbenes versus lignin decides the outcome of plant–fungal interaction (Khattab et al., 2021). In fact, we could show that feeding a specific precursor of monolignols, ferulic acid, induced the fungus to release phytotoxins (Figure 2d–f). Interestingly, cinnamic and coumaric acid, situated upstream of ferulic acid in the pathway, did not induce phytotoxicity. In contrast, they downmodulate the innate toxicity of the fungal culture filtrate (Figure 2e). Since coumaric acid is also the branching point for the stilbene synthesis, a high steady-state level of coumaric acid would report the efficient synthesis of stilbenes, and thus, would report host vigour. The same holds true, less tightly, for cinnamic acid (in fact, cinnamic acid silences phytotoxin release as well, albeit less efficiently compared to coumaric acid). The first metabolite committed for monolignols is caffeic acid (www.kegg.jp, search vvi, ferulate). Thus, an increase in the steady-state levels of caffeic acid would report a bottleneck in lignin synthesis and qualify as a readout for the fungus to detect a serious host crisis. Interestingly, and unexpectedly, this is not what we observe: 'caffeic acid' quells phytotoxicity almost as efficiently as its precursor, coumaric acid. The key to this enigma may be the enzyme 4-coumarate ligase (gene VIT_16s0039g02040, protein UniProt F6HEF8), which is very permissive and accepts any phenolic acid as substrate (cinnamic acid, coumaric acid, caffeic acid, ferulic acid, 5-hydroxy ferulic acid (F5H) and even the monolignol sinapic acid; www.kegg.jp) to confer a coenzyme A residue for further metabolization. Any change in the activity of this enzyme would, therefore, result in a complete shutdown of the entire pathway, and thus, is not apt to act as a lever to sense changes in stilbene versus lignin partitioning. However, there exists an enzyme, specifically recruiting ferulic acid for monolignol synthesis: the cytochrome P_{450} 84A1 enzyme ferulate-5-hydroxylase (in grapevine present in tandem as gene VIT_03s0038g00500, protein UniProt D7U5I5 and the almost identical gene VIT_03s0038g00550, protein UniProt F6I194). Ferulate-5-hydroxylase is the rate-limiting enzyme for monolignols synthesis and as such strongly regulated (Ruegger et al., 1999). The fact that this enzyme was among the most pertinent candidates during a transcriptomics study either in *V. vinifera* infected with *N. parvum* or even in Chinese wild grapes infected with *Plasmopara viticola* (Liu et al., 2019; Massonnet et al., 2017) could indicate that this gene is subject to tight regulation. The rice homolog of F5H is strongly down-regulated under drought (tenor.dna.affrc.go.jp, search Os06g0349700), especially in roots. Whether this holds true for grapevine as well is not known, but would represent a testable implication of the surrender signal model.

4.3 | What is the functional context of FCA-triggered PCD?

Our data introduce the new concept of 'surrender signal' into models of plant–pathogen dialogue (Figure 10). While healthy plants accumulate coumaric acid, a precursor of bioactive stilbenes, whose antifungal properties are able to protect the plant, under climate-born stress or drought, the monolignol precursor ferulic acid accumulates, signalling to the fungus that the plant is under severe stress. In response, the fungus will convert ferulic acid into vanillic acid (Shimizu et al., 2005), which might trigger the transition to sexual development and necrotrophy (culminating in apoplexy) through the secretion of phytotoxins, such as FCA, to kill the host and to allow to complete *N. parvum* lifecycle (Figure 10,①,②). After binding to 14-3-3 proteins (Figure 10,③), FCA triggers extracellular acidification via binding to PM ATPases in a few minutes (Kinoshita & Shimazaki, 2001; Figure 10,④), which could trigger cell wall loosening enzymes supporting cell-wall degradation (Kesten et al., 2019). The acidification will also activate RbOH (Huang et al., 2014; Majumdar & Kar, 2018) after 10 min reaching the peak after 60 min (Figure 10,⑤).

Here, superoxide O_2^- acts as an upstream signal to trigger FCA stress signalling, since blocking RboH by DPI reduced the FCA-dependent PCD, similar to earlier observations in sycamore cells (Malerba et al., 2008). This is followed by microtubule breakdown from 30 min of FCA treatment (Figure 10,⑥). Microtubules act as negative regulators of signalling, possibly by tethering metacaspases and/or 14-3-3 proteins (Pignocchi & Doonan, 2011), similar to their role in self-incompatibility (Poulter et al., 2008). In addition, metacaspases 5, a central regulator of the hypersensitive response in grapevine (Gong et al., 2019) has been shown to be tethered (and possibly restrained) on microtubules Zhu (2020). The breakdown of microtubules might unleash the executors of cell death. If so, taxol pretreatment would be predicted to mitigate cell death. This is not, what we observe (Figure 7d). Alternatively, microtubules, through their amplifying activity in the opening of calcium influx channels, might repress PCD indirectly by promoting basal immunity (Nick et al., 2021). Subsequently, from 90 min of FCA treatment, actin responds by strong remodelling (Figure 10,⑦). While actin remodelling accompanies PCD in many systems (Smertenko and Tong, 2011), it does not induce PCD per se. The recruitment of 14-3-3 proteins might be the cause for the PM ATPases to release metacaspases too. In fact, overexpression of Type-II metacaspases in poplar reduces the abundance of 14-3-3 proteins, indicating a functional interaction (Bollhöner et al., 2018). Thus, activation of metacaspases might then trigger the expression of metacaspase genes (Figure 10,⑧) sustaining PCD execution (Tsiatsiani et al., 2011; Figure 10,⑨). Nevertheless, FCA-triggered cell death was independent of MAPK cascades, which were found to be linked to PAMP-triggered immunity, rather than to PCD in grapevine cells (Duan et al., 2016). By contrast, manipulating SA signalling, which is more linked to effector-triggered immunity (Armijo et al., 2013) altered FCA toxicity, meaning that FCA signalling would target the PCD directly. Interestingly, most pharmacological treatments mitigating FCA toxicity reduced the accumulated transcripts of genes regulating SA signalling, *PAL* and *PR1*, and increased the transcripts of a competitive pathway *STS27* and *STS47*. Here, we arrived at a conclusion that the phenylpropanoid pathway might act as a lever for the disturbing actions of FCA. Several, partially nonintuitive implications of this model have been tested and

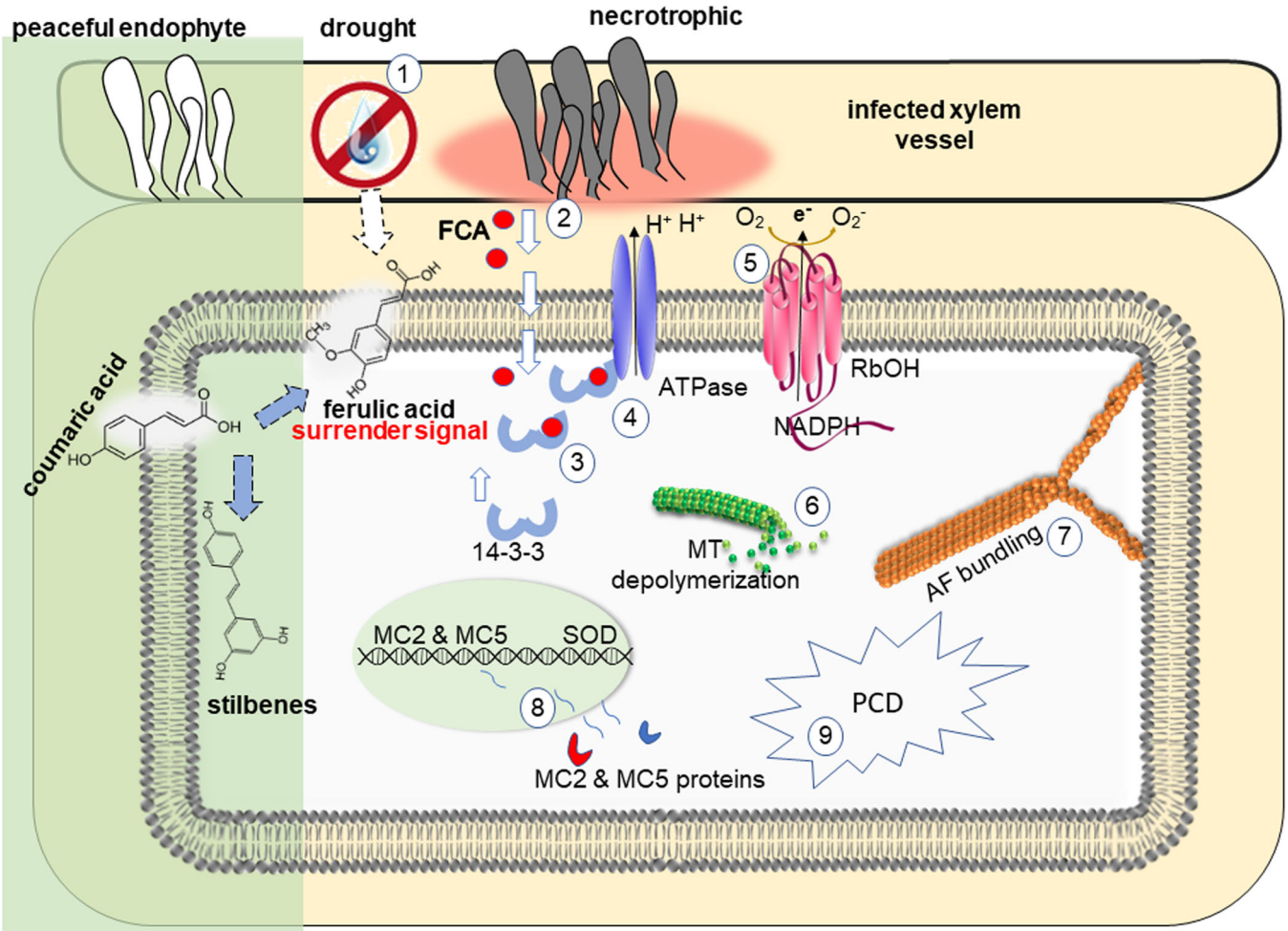

FIGURE 10 Working model showing the chemical communication driving apoplexy in *Botryosphaeriaceae–Vitis* interaction and the stress signalling induced by the apoplexy signal (fusicoccin A) [Color figure can be viewed at wileyonlinelibrary.com]

confirmed. A rapid oxidative burst inhibited the responses of DPI, (destabilizing actin), latrunculin (stabilizing microtubules) and taxol and also reduced mortality in cells overexpressing GFP-tagged tubulin.

4.4 | Outlook: What does this model contribute to a potential therapy against Botryosphaeria dieback

The outputs of this study pave the way for sustainable applications to control GTD by preventing the pathogen to hijack the derivatives of the phenylpropanoid pathway to ensure its own aggressiveness. Of course, it will be necessary to validate the phenomena seen in cell cultures and also in planta; for instance, by assessing the correlation between ferulic acid under drought and apoplexy, or to quantify FCA in infected vines. However, already at this stage, the concepts and findings developed in this study stimulate hypothesis-driven application. At least two approaches can be conceived: (i) chemical genetics as an immediate strategy to contain disease outbreaks to bridge the time until new resistant varieties become available. In this approach, compound libraries (van de Wouwer et al., 2016) will be used to modulate the pathway to avoid the accumulation of ferulic acid. (ii) Marker-assisted breeding based on genome sequencing of the almost entire population of the ancestral European wild grapevine (Liang et al., 2019), which contains the spread of GTDs (Khattab et al., 2021).

ACKNOWLEDGEMENTS

This study was supported by the European Fund (Interreg Upper Rhine, projects Vitifutur and DialogProTec). I. M. K. was awarded also a full PhD scholarship from the German Egyptian Research Long-term Scholarships DAAD-GERLS programme in addition to the DAAD STIBET grant to complete this study. Open Access funding enabled and organized by Projekt DEAL.

DATA AVAILABILITY STATEMENT

The data that support the findings of this study are available from the corresponding author upon reasonable request.

ORCID

Islam M. Khattab http://orcid.org/0000-0003-2370-0766
Peter Nick http://orcid.org/0000-0002-0763-4175

REFERENCES

Abou-Mansour, E., Débieux, J.-L., Ramírez-Suero, M., Bénard-Gellon, M., Magnin-Robert, M., Spagnolo, A., Chong, J., Farine, S., Bertsch, C., L'Haridon, F., Serrano, M., Fontaine, F., Rego, C. & Larignon, P. (2015) Phytotoxic metabolites from neofusicoccum parvum, a pathogen of botryosphaeria dieback of grapevine. *Phytochemistry*, 115, 207–215. https://doi.org/10.1016/j.phytochem.2015.01.012

Akaberi, S., Wang, H., Claudel, P., Riemann, M., Hause, B., Hugueney, P. et al. (2018) Grapevine fatty acid hydroperoxide lyase generates actin-disrupting volatiles and promotes defence-related cell death. *Journal of Experimental Botany*, 69, 2883–2896.

Andolfi, A., Mugnai, L., Luque, J., Surico, G., Cimmino, A. & Evidente, A. (2011) Phytotoxins produced by fungi associated with grapevine trunk diseases. *Toxins*, 3, 1569–1605. Available from: https://doi.org/10.3390/toxins3121569

Armijo, G., Salinas, P., Monteoliva, M.I., Seguel, A., García, C., Villarroel-Candia, E. et al. (2013) A salicylic acid-induced lectin-like protein plays a positive role in the effector-triggered immunity response of *Arabidopsis thaliana* to pseudomonas syringae Avr-Rpm1. *Molecular Plant-Microbe Interactions*, 26(12), 1395–1406. Available from: https://doi.org/10.1094/MPMI-02-13-0044-R

Bollhöner, B., Jokipii-Lukkari, S., Bygdell, J., Stael, S., Adriasola, M., Muñiz, L. et al. (2018) The function of two type II metacaspases in woody tissues of Populus trees. *New Phytologist*, 217(4), 1551–1565.

Bortolami, G., Gambetta, G.A., Delzon, S., Lamarque, L.J., Pouzoulet, J., Badel, E. et al. (2019) Exploring the hydraulic failure hypothesis of Esca leaf symptom formation 1. *Plant Physiology*, 181(11), 1163–1174.

Buckel, I., Andernach, L., Schüffler, A., Piepenbring, M., Opatz, T. & Thines, E. (2017) Phytotoxic dioxolanones are potential virulence factors in the infection process of *Guignardia bidwellii*. *Scientific Reports*, 7(1), 8926.

Byczkowska, A., Kunikowska, A. & Kaźmierczak, A. (2013) Determination of ACC-induced cell-programmed death in roots of *Vicia faba* ssp. minor seedlings by acridine orange and ethidium bromide staining. *Protoplasma*, 250(1), 121–128.

Carlucci, A., Cibelli, F., Lops, F. & Raimondo, M.L. (2015) Characterization of *Botryosphaeriaceae* species as causal agents of trunk diseases on grapevines. *Plant Disease*, 99(12), 1678–1688.

Chang, X., Heene, E., Qiao, F. & Nick, P. (2011) The phytoalexin resveratrol regulates the initiation of hypersensitive cell death in *Vitis* cell. *PLoS One*, 6(10), 26405.

Chang, X. & Nick, P. (2012) Defence signalling triggered by Flg22 and harpin is integrated into a different stilbene output in *Vitis* cells. *PLoS One*, 7(7), 40446.

Chang, X., Riemann, M., Liu, Q. & Nick, P. (2015) Actin as deathly switch? How auxin can suppress cell-death related defence. *PLoS One*, 10(5), 1–22.

Chuberre, C., Plancot, B., Driouich, A., Moore, J.P., Bardor, M., Gügi, B. & Vicré, M. (2018) Plant immunity is compartmentalized and specialized in roots. *Frontiers in Plant Science*, 871(November), 1–13. https://doi.org/10.3389/fpls.2018.01692

Claverie, M., Notaro, M., Fontaine, F. & Wery, J. (2020) Current knowledge on grapevine trunk diseases with complex etiology: a systemic approach. *Phytopathologia Mediterranea*, 59, 29–53.

Cota-Sánchez, J.H., Remarchuk, K. & Ubayasena, K. (2006) Ready-to-use DNA extracted with a CTAB method adapted for herbarium specimens and mucilaginous plant tissue. *Plant Molecular Biology Reporter*, 24(2), 161–167. https://doi.org/10.1007/BF02914055

Delaye, L., García-Guzmán, G. & Heil, M. (2013) Endophytes versus biotrophic and necrotrophic pathogens-are fungal lifestyles evolutionarily stable traits? *Fungal Diversity*, 60(1), 125–135. Available from: https://doi.org/10.1007/s13225-013-0240-y

Djoukeng, J.D., Polli, S., Larignon, P. & Abou-Mansour, E. (2009) Identification of phytotoxins from *Botryosphaeria obtusa*, a pathogen of black dead arm disease of grapevine. *European Journal of Plant Pathology*, 124(2), 303–308.

Duan, D., Fischer, S., Merz, P., Bogs, J., Riemann, M. & Nick, P. (2016) An ancestral allele of grapevine transcription factor MYB14 promotes plant defence. *Journal of Experimental Botany*, 67(6), 1795–1804. Available from: https://doi.org/10.1093/jxb/erv569

Faulds, C.B., Molina, R., Gonzalez, R., Husband, F., Juge, N., Sanz-Aparicio, J. et al. (2005) Probing the determinants of substrate specificity of a feruloyl esterase, AnFaeA, from *Aspergillus niger*. *FEBS Journal*, 272(17), 4362–4371.

Flubacher, N.S. (2021) *4-Hydroxyphenylacetic acid—a fungal polyketide suppressing plant defence*. Dissertation. Karlsruhe Institute of Technology, Germany.

Gaff, D., Okong'o-Ogola, O. (1971) The use of non-permeating pigments for testing the survival of cells. *Journal of Experimental Botany*, 22, 756–758.

Galarneau, E.R.A., Lawrence, D.P., Travadon, R. & Baumgartner, K. (2019) Drought exacerbates Botryosphaeria dieback symptoms in grapevines and confounds host-based molecular markers of infection by *Neofusicoccum parvum*. *Plant Disease*, 103(7), 1738–1745.

Gómez, P., Báidez, A.G., Ortuño, A. & Del Río, J.A. (2016) Grapevine xylem response to fungi involved in trunk diseases. *Annals of Applied Biology*, 169(1), 116–124.

Gong, P., Riemann, M., Dong, D., Stoeffler, N., Gross, B., Markel, A. et al. (2019) Two grapevine metacaspase genes mediate ETI-like cell death in grapevine defence against infection of *Plasmopara viticola*. *Protoplasma*, 256(4), 951–969.

Griesser, M., Weingart, G., Schoedl-Hummel, K., Neumann, N., Becker, M., Varmuza, K. et al. (2015) Severe drought stress is affecting selected primary metabolites, polyphenols, and volatile metabolites in grapevine leaves (*Vitis vinifera* cv. Pinot noir). *Plant Physiology and Biochemistry*, 88, 17–26.

Guan, P., Terigele, Schmidt, F., Riemann, M., Fischer, J. & Thines, E. et al. (2020) Hunting modulators of plant defence-the grapevine trunk disease fungus *Eutypa lata* secretes an amplifier for plant basal immunity. *Journal of Experimental Botany*, 71, 3710–3724.

Guan, P.Y., Schmidt, F., Fischer, J., Riemann, M., Thines, E. & Nick, P. (2022) The fungal elicitor eutypine from *Eutypa lata* activates basal immunity through its phenolic side chains. *Horticultural Research*, 9, uhac120. Available from: https://doi.org/10.1093/hr/uhac120

Guan, X., Buchholz, G. & Nick, P. (2015) Tubulin marker line of grapevine suspension cells as a tool to follow early stress responses. *Journal of Plant Physiology*, 176, 118–128.

Guan, X., Essakhi, S., Laloue, H., Nick, P., Bertsch, C. & Chong, J. (2016) Mining new resources for grape resistance against *Botryosphaeriaceae*: a focus on *Vitis vinifera* subsp. *sylvestris*. *Plant Pathology*, 65(2), 273–284.

Harris, S.D. (2009) The Spitzenkörper: a signalling hub for the control of fungal development? *Molecular Microbiology*, 73(5), 733–736.

Hofstetter, V., Buyck, B., Croll, D., Viret, O., Couloux, A. & Gindro, K. (2012) What if Esca disease of grapevine were not a fungal disease? *Fungal Diversity*, 54(May), 51–67.

Huang, A.X., She, X.P., Zhao, J.L. & Zhang, Y.Y. (2014) Inhibition of ABA-induced stomatal closure by fusicoccin is associated with cytosolic acidification-mediated hydrogen peroxide removal. *Botanical Studies*, 55(1), 1–11. Available from: https://doi.org/10.1186/1999-3110-55-33

Jones, J. & Dangl, J. (2006) The plant immune system. *Nature*, 444, 323–329.

Kesten, C., Gámez-Arjona, F.M., Menna, A., Scholl, S., Dora, S., Huerta, A.I. & Huang, H.-Y. et al. (2019) Pathogen-induced pH changes regulate the growth-defense balance in plants. *The EMBO Journal*, 38(24), 1–20. Available from: https://doi.org/10.15252/embj.2019101822

Khattab, I.M., Sahi, V.P., Baltenweck, R., Maia-Grondard, A., Hugueney, P., Bieler, E. et al. (2021) Ancestral chemotypes of cultivated grapevine with resistance to *Botryosphaeriaceae*-related dieback allocate metabolism towards bioactive stilbenes. *New Phytologist*, 229(2), 1133–1146.

Kinoshita, T. & Shimazaki, K.I. (2001) Analysis of the phosphorylation level in guard-cell plasma membrane H+-ATPase in response to fusicoccin. *Plant and Cell Physiology*, 42(4), 424–432.

Labois, C., Wilhelm, K., Laloue, H., Tarnus, C., Bertsch, C. & Goddard, et al. (2020) Wood metabolomic responses of wild and cultivated grapevine to infection with *Neofusicoccum parvum*, a trunk disease pathogen. *Metabolites*, 10(6), 232. Available from: https://doi.org/10.3390/metabo10060232

Leal, C., Richet, N., Guise, J.F., Gramaje, D., Armengol, J. & Fontaine, F. et al. (2021) Cultivar contributes to the beneficial effects of *Bacillus subtilis* PTA-271 and *Trichoderma atroviride* SC1 to protect grapevine against *Neofusicoccum parvum*. *Frontiers in Microbiology*, 12(Octo-October), 1–17. Available from: https://doi.org/10.3389/fmicb.2021.726132

Leon, J., Shulaev, V., Yalpani, N., Lawton, M.A. & Raskint, I. (1995) Benzoic acid 2-hydroxylase, a soluble oxygenase from tobacco, catalyzes salicylic acid biosynthesis (*Nicotiana tabacum*/tobacco mosaic virus/cytochrome P450/acquired resistance). *Plant Biology*, 92(October), 10413–10417.

Liang, Z., Duan, S., Sheng, J., Zhu, S., Ni, X., Shao, J. et al. (2019) Whole-genome resequencing of 472 *Vitis* accessions for grapevine diversity and demographic history analyses. *Nature Communications*, 10(1), 1–12.

Lima, M.R.M., Machado, A.F. & Gubler, W.D. (2017) Metabolomic study of Chardonnay grapevines double stressed with Esca-associated fungi and drought. *Phytopathology*, 107(6), 669–680.

Liu, R., Weng, K., Dou, M., Chen, T., Yin, X., Li, Z. et al. (2019) Transcriptomic analysis of Chinese wild *Vitis pseudoreticulata* in response to *Plasmopara viticola*. *Protoplasma*, 256, 1409–1424.

Livak, K.J. & Schmittgen, T.D. (2001) Analysis of relative gene expression data using real-time quantitative PCR and the 2(−Delta Delta C(T)) method. *Methods*, 25, 402–408.

Loeffler, F. (1884) Untersuchung über die Bedeutung der Mikroorganismen für die Entstehung der Diphtherie beim Menschen, bei der Taubetaube und beim Kalbe. *Mittheilungen kaiserl Gesundheitsamt*, 2, 421–499.

Majumdar, A. & Kar, R.K. (2018) Congruence between PM H^+-ATPase and NADPH oxidase during root growth: a necessary probability. *Protoplasma*, 255(4), 1129–1137.

Malerba, M., Cerana, R. & Crosti, P. (2004) Comparison between the effects of fusicoccin, tunicamycin, and brefeldin A on programmed cell death of cultured sycamore (*Acer pseudoplatanus* L.) cells. *Protoplasma*, 224(1–2), 61–70. Available from: https://doi.org/10.1007/s00709-004-0053-7

Malerba, M., Contran, N., Tonelli, M., Crosti, P. & Cerana, R. (2008) Role of nitric oxide in actin depolymerization and programmed cell death induced by fusicoccin in sycamore (*Acer pseudoplatanus*) cultured cells. *Physiologia Plantarum*, 133(2), 449–457.

Masi, M., Reveglia, P., Femina, G., Baaijens-Billones, R., Savocchia, S. & Evidente, A. (2020) Luteoethanones A and B, two phytotoxic 1-substituted ethanones produced by Neofusicoccum luteum, a causal agent of Botryosphaeria dieback on grapevine. *Natural Product Research*, 1–8. https://doi.org/10.1080/14786419.2020.1739045

Massonnet, M., Figueroa-Balderas, R., Galarneau, E.R.A., Miki, S., Lawrence, D.P., Sun, Q. et al. (2017) *Neofusicoccum parvum* colonization of the grapevine woody stem triggers asynchronous host responses at the site of infection and in the leaves. *Frontiers in Plant Science*, 8(June), 1117.

Mugnai, L., Graniti, A. & Surico, G. (1999) Esca (black measles) and brown wood-streaking: two old and elusive diseases of grapevines. *Plant Disease*, 83(5), 404–418.

Nick, P., Guan, P., Shi, W.J. & Riemann, M. (2021) Dissecting the membrane-microtubule sensor in grapevine defence. *Horticulture Research*, 8, 260.

Pescitelli, G., Masi, M., Reveglia, P., Baaijens-billones, R., Go, M., Savocchia, S. & Evidente, A. (2020) Phytotoxic metabolites from three neofusicoccum species causal agents of botryosphaeria dieback in Australia, luteopyroxin, neoanthraquinone, and luteoxepinone, a disubstituted furo-α- pyrone, a hexasubstituted

anthraquinone, and a trisubstituted oxepi-2-. *Journal of Natural Products*, 83, 453–460. https://doi.org/10.1021/acs.jnatprod.9b01057

Pietrowska, E., Różalska, S., Kaźmierczak, A., Nawrocka, J. & Małolepsza, U. (2014) Reactive oxygen and nitrogen (ROS and RNS) species generation and cell death in tomato suspension cultures–*Botrytis cinerea* interaction. *Protoplasma*, 252(1), 307–319.

Pignocchi, C. & Doonan, J.H. (2011) Interaction of a 14-3-3 protein with the plant microtubule-associated protein EDE1. *Annals of Botany*, 107(7), 1103–1109.

Piscitelli, A., Giardina, P., Lettera, V., Pezzella, C., Sannia, G. & Faraco, V. (2011) Induction and transcriptional regulation of laccases in fungi. *Current Genomics*, 12(2), 104–112.

Pitt, W.M., Huang, R., Steel, C.C. & Savocchia, S. (2013) Pathogenicity and epidemiology of *Botryosphaeriaceae* species isolated from grapevines in Australia. *Australasian Plant Pathology*, 42(5), 573–582. Available from: https://doi.org/10.1007/s13313-013-0221-3

Poulter, N.S., Vatovec, S. & Franklin-Tong, V.E. (2008) Microtubules are a target for self-incompatibility signaling in Papaver pollen. *Plant Physiology*, 146(3), 1358–1367.

Pouzoulet, J., Scudiero, E., Schiavon, M. & Rolshausen, P.E. (2017) Xylem vessel diameter affects the compartmentalization of the vascular pathogen *Phaeomoniella chlamydospora* in grapevine. *Frontiers in Plant Science*, 8, 1–13.

Qiao, F., Chang, X.L. & Nick, P. (2010) The cytoskeleton enhances gene expression in the response to the Harpin elicitor in grapevine. *Journal of Experimental Botany*, 61(14), 4021–4031.

Ramírez-Suero, M., Bénard-Gellon, M., Chong, J., Laloue, H., Stempien, E., Abou-Mansour, E., Fontaine, F., Larignon, P., Mazet-Kieffer, F., Farine, S. & Bertsch, C. (2014) Extracellular compounds produced by fungi associated with Botryosphaeria dieback induce differential defence gene expression patterns and necrosis in Vitis vinifera cv. Chardonnay cells. *Protoplasma*, 251(6), 1417–1426. https://doi.org/10.1007/s00709-014-0643-y

Reis, P., Magnin-Robert, M., Nascimento, T., Spagnolo, A., Abou-Mansour, E., Fioretti, C. et al. (2016) Reproducing Botryosphaeria dieback foliar symptoms in a simple model system. *Plant Disease*, 100, 1071–1079.

Reveglia, P., Billones-baaijens, R., Niem, J.M., Masi, M., Cimmino, A., Evidente, A. et al. (2021) Production of phytotoxic metabolites by *Botryosphaeriaceae* in naturally infected and artificially inoculated grapevines. *Plants*, 10(4), 1–17. Available from: https://doi.org/10.3390/plants10040802

Ridgway, H.J., Amponsah, N.T., Brown, D.S., Baskarathevan, J., Jones, E.E. & Jaspers, M.V. (2011) Detection of botryosphaeriaceous species in environmental samples using a multi-species primer pair. *Plant Pathology*, 60(6), 1118–1127. https://doi.org/10.1111/j.1365-3059.2011.02474.x

Ruegger, M., Meyer, K., Cusumano, J.C. & Chapple, C. (1999) Regulation of Ferulate-5-hydroxylase expression in *Arabidopsis* in the context of sinapate ester biosynthesis. *Plant Physiology*, 119, 101–110.

Schwarzerová, K., Zelenková, S., Nick, P. & Opatrný, Z. (2002) Aluminum-induced rapid changes in the microtubular cytoskeleton of tobacco cell lines. *Plant and Cell Physiology*, 43(2), 207–216.

Shimizu, M., Kobayashi, Y., Tanaka, H. & Wariishi, H. (2005) Transportation mechanism for vanillin uptake through fungal plasma membrane. *Applied Microbiology and Biotechnology*, 68(5), 673–679.

Singh, J. & Roberts, M.R. (2004) Fusicoccin activates pathogen-responsive gene expression independently of common resistance signalling pathways, but increases disease symptoms in *Pseudomonas syringae*-infected tomato plants. *Planta*, 219(2), 261–269. Available from: https://doi.org/10.1007/s00425-004-1234-5

Slippers, B. & Wingfield, M.J. (2007) Botryosphaeriaceae as endophytes and latent pathogens of woody plants: diversity, ecology and impact. *Fungal Biology Reviews*, 21(2–3), 90–106.

Smertenko, A. & Franklin-Tong, V.E. (2011) Organisation and regulation of the cytoskeleton in plant programmed cell death. *Cell Death and Differentiation*, 18(8), 1263–1270. https://doi.org/10.1038/cdd.2011.39

Steffens, B. & Sauter, M. (2009) Epidermal cell death in rice is confined to cells with a distinct molecular identity and is mediated by ethylene and H_2O_2 through an autoamplified signal pathway. *The Plant Cell*, 21(1), 184–196.

Stempien, E., Goddard, M.L., Wilhelm, K., Tarnus, C., Bertsch, C. & Chong, J. (2017) Grapevine Botryosphaeria dieback fungi have specific aggressiveness factor repertory involved in wood decay and stilbene metabolization. *PLoS One*, 12(12), 1–22.

Stevers, L.M., Sijbesma, E., Botta, M., Mackintosh, C., Obsil, T., Landrieu, I. et al. (2018) Modulators of 14-3-3 protein–protein interactions. *Journal of Medicinal Chemistry*, 61(9), 3755–3778.

Svyatyna, K., Jikumaru, Y., Brendel, R., Reichelt, M., Mithöfer, A., Takano, M. et al. (2014) Light induces jasmonate–isoleucine conjugation via OsJAR1-dependent and -independent pathways in rice. *Plant, Cell and Environment*, 37(4), 827–839.

Toyomasu, T., Tsukahara, M., Kaneko, A., Niida, R., Mitsuhashi, W., Dairi, T. et al. (2007) Fusicoccins are biosynthesized by an unusual chimera diterpene synthase in fungi. *Proceedings of the National Academy of Sciences of the United States of America*, 104(9), 3084–3088.

Trotel-Aziz, P., Robert-Siegwald, G., Fernandez, O., Leal, C., Villaume, S., Guise, J.-F. et al. (2022) Diversity of *Neofusicoccum parvum* for the production of the phytotoxic metabolites (−)-terremutin and (*R*)-mellein. *Journal of Fungi*, 8(3), 319. Available from: https://doi.org/10.3390/jof8030319

Tsiatsiani, L., Van Breusegem, F., Gallois, P., Zavialov, A., Lam, E. & Bozhkov, P.V. (2011) Metacaspases. *Cell Death and Differentiation*, 18(8), 1279–1288. Available from: https://doi.org/10.1038/cdd.2011.66

Tu, M., Wang, X., Yin, W., Yin, W., Wang, Y., Li, Y. et al. (2020) Grapevine VlbZIP30 improves drought resistance by directly activating VvNAC17 and promoting lignin biosynthesis through the regulation of three peroxidase genes. *Horticultural Research*, 7, 150.

Umezawa, T. (2010) The cinnamate/monolignol pathway. *Phytochemistry Reviews*, 9(1), 1–17. Available from: https://doi.org/10.1007/s11101-009-9155-3

Úrbez-Torres, J.R. (2011) The status of *Botryosphaeriaceae* species infecting grapevines José. *Phytopathologia Mediterranea*, 50(4), 5–45.

Úrbez-Torres, J.R. & Gubler, W.D. (2009) Pathogenicity of *Botryosphaeriaceae* species isolated from grapevine cankers in California. *Plant Disease*, 93(6), 584–592.

Wang, L. & Nick, P. (2017) Cold sensing in grapevine—which signals are upstream of the microtubular "thermometer". *Plant Cell and Environment*, 40(11), 2844–2857. https://doi.org/10.1111/pce.13066

Wang, R., Duan, D., Metzger, C., Zhu, X., Riemann, M., Pla, M. et al. (2022) Aluminum can activate grapevine defense through actin remodeling. *Horticulture Research*, 9, 016. Available from: https://doi.org/10.1093/hr/uhab016

Watanabe, N. & Lam, E. (2011) *Arabidopsis* metacaspase 2d is a positive mediator of cell death induced during biotic and abiotic stresses. *Plant Journal*, 66(6), 969–982.

van de Wouwer, D., Vanholme, R., Decou, R., Goeminne, G., Audenaert, D., Nguyen, L. et al. (2016) Chemical genetics uncovers novel inhibitors of lignification, including *p*-iodobenzoic acid targeting CINNAMATE-4-HYDROXYLASE. *Plant Physiology*, 172(1), 198–220.

Zhu, X. (2020) *Green leaf volatile triggered defense signalling and cell death mediated by Vitis metacaspase 5*. PhD thesis. Karlsruhe Institute of Technology, Germany.

SUPPORTING INFORMATION

Additional supporting information can be found online in the Supporting Information section at the end of this article.

How to cite this article: Khattab, I. M., Fischer, J., Kaźmierczak, A., Thines, E. & Nick, P. (2023) Ferulic acid is a putative surrender signal to stimulate programmed cell death in grapevines after infection with *Neofusicoccum parvum*. *Plant, Cell & Environment*, 46, 339–358. https://doi.org/10.1111/pce.14468